Bioorganic & Medicinal Chemistry 24 (2016) 2725–2738

Contents lists available at ScienceDirect

Bioorganic & Medicinal Chemistry

journal homepage: www.elsevier.com/locate/bmc

Synthesis and inhibitory evaluation of 3-linked imipramines for the exploration of the S2 site of the human serotonin transporter

Anne Brinkø [a,†], Maja T. Larsen [b,†], Heidi Koldsø [a,c,†,‡], Louise Besenbacher [a], Anders Kolind [b], Birgit Schiøtt [a,c], Steffen Sinning [b,*], Henrik H. Jensen [a,*]

[a] Department of Chemistry, Aarhus University, Denmark
[b] Laboratory of Molecular Neurobiology, Translational Neuropsychiatry Unit, Department of Clinical Medicine, Aarhus University, Risskov, Denmark
[c] inSPIN & iNANO Centres, Langelandsgade 140, 8000 Aarhus C, Denmark

ARTICLE INFO

Article history:
Received 19 November 2015
Revised 16 April 2016
Accepted 20 April 2016
Available online 21 April 2016

Keywords:
Antidepressants
Sonogashira coupling
Bivalent ligands
Serotonin
Transporter
Depression

ABSTRACT

The human serotonin transporter is the primary target of several antidepressant drugs, and the importance of a primary, high affinity binding site (S1) for antidepressant binding is well documented. The existence of a lower affinity, secondary binding site (S2) has, however, been debated. Herein we report the synthesis of 3-position coupled imipramine ligands from clomipramine using a copper free Sonogashira reaction. Ligand design was inspired by results from docking and steered molecular dynamics simulations, and the ligands were utilized in a structure–activity relationship study of the positional relationship between the S1 and S2 sites. The computer simulations suggested that the S2 site does indeed exist although with lower affinity for imipramine than observed within the S1 site. Additionally, it was possible to dock the 3-linked imipramine analogs into positions which occupy the S1 and the S2 site simultaneously. The structure activity relationship study showed that the shortest ligands were the most potent, and mutations enlarging the proposed S2 site were found to affect the larger ligands positively, while the smaller ligands were mostly unaffected.

1. Introduction

The human serotonin transporter (hSERT) belongs to the Neurotransmitter: Sodium Symporters (NSS) family and it regulates the synaptic concentration of serotonin in the brain by reuptake of serotonin.[1,2] The transporter thus plays a critical role in modulating important physiological functions such as mood, appetite, and sleep.[2] hSERT is the primary target of several antidepressant drugs belonging to the class of selective serotonin reuptake inhibitors (SSRIs) such as citalopram and sertraline, but also less selective drugs from the tricyclic antidepressants class (TCAs) such as clomipramine and imipramine.[2] These drugs inhibit hSERT regulated reuptake of serotonin from the synaptic cleft, effectively raising the concentration of serotonin available to the brain, thus relieving the symptoms of depression through a still unknown mechanism.[3]

Even though pharmacological treatment of depression has come a long way, it still suffers from several challenges, such as latency periods of 3–4 weeks, a range of severe side effects, and a high percentage of non-responding patients.[4] As a result, research into the fundamental underlying mechanism of hSERT and its regulation remains an important and active area of research.[2,5] Resolution of a crystal structure of the bacterial (*Aquifex aeolicus*) amino acid transporter $LeuT_{Aa}$[6] has made it possible to construct a homology model of hSERT[7,8] with the primary (S1) binding pocket occupied by imipramine,[9,10] escitalopram,[10,11] mazindol,[12] fluoxetine,[13] phenylpiperazine,[14] cocaine,[15] noribogaine[15] and serotonin.[16,17] The TCA clomipramine and the SSRIs fluoxetine and sertraline have, however, been found to bind in an extracellular vestibule termed the S2 binding site of the bacterial protein $LeuT_{Aa}$.[18,19] Data supporting the existence of a similar S2 site in hSERT have been published,[20–23] but its role in transport and transport inhibition has been debated. It has been shown that the S2 site might play an allosteric role in the pharmacological action of serotonin itself.[24] Binding to the S2 site can also affect the pharmacological properties of some SSRIs and TCAs, in particular imipramine, where binding to the S2 site can modulate the dissociation rate from hSERT.[24] A detailed study has revealed that the S2 site might be located in an extracellular vestibule approximately 10–12 Å above the S1

* Corresponding authors.
E-mail addresses: steffen.sinning@clin.au.dk (S. Sinning), hhj@chem.au.dk (H.H. Jensen).
† These authors contributed equally.
‡ Present address: D. E. Shaw Research, 120 W. 45th St., 39th Fl. New York, NY 10036, United States.

http://dx.doi.org/10.1016/j.bmc.2016.04.039
0968-0896/

binding site, and it has been suggested that the modulation of dissociation rate via an allosteric site is due to a steric blockage of the exit pathway caused by the low-affinity binding of antidepressants to the S2 site.[20]

The suggested existence of a S2 site in hSERT with affinity for antidepressants indicates that it may be possible to synthesize ligands that are dimeric or bifunctional in nature, and so could occupy both S1 and S2 binding sites simultaneously. Literature holds several examples of dimeric inhibitors, or inhibitors with two interlinked binding motifs, showing improved affinity compared to the single binder,[25–30] and so a dimeric/bifunctional antidepressant might possess improved binding affinity and selectivity compared to other known antidepressant drugs. In a recent study it was shown that citalopram analogs linked either symmetrically through the 5-position or un-symmetrically linked through the N- and 5-position lost affinity compared to S-citalopram but retained nanomolar affinity. Some of these dimeric compounds were still able to bind to the S1 and to the allosteric site and even exhibited improved allosteric properties, however, it remains unclear whether their binding utilized both S1 and S2 simultaneously.[31]

In order to explore the possibility of targeting hSERT with a ligand binding to both the S1 and S2 binding sites, we performed computational studies which suggested that a well-defined binding site is located in an extracellular vestibule, approximately 10–12 Å from the S1 site. Accordingly, if an S2 site exists it will likely be situated in this vestibule, consistent with previously published studies.[9,20,32] We have formerly biochemically validated a computational study that placed imipramine in the primary S1 binding site orientated in such a way that the 3-position (Fig. 1) was directed towards the exit of the binding pocket, in the direction of the extracellular vestibule[9,33] and shown that extended substituents are tolerated at this position.[37] This binding location and orientation has recently been confirmed by Gouaux and co-workers using crystal structures of dDAT and a mutated LeuT.[18,19] Given the confidence we now have in our SERT model of imipramine binding we set out to explore the existence and position of the debated S2 site by synthesizing a series of ligands that could target both binding sites, and experimentally challenge or support the computational results. We decided to use iminodibenzyl fragments to probe S2 because earlier studies have shown that tricyclic antidepressants bind to the S2 site of LeuT.[21,38] Furthermore, because the putative S2 site is expected to be smaller in hSERT we also employed naphthyl fragments.

In this paper we report on both computational and experimental data supporting an S2 site to be located approximately 10–12 Å from the S1 site, similar to what was observed from steered molecular dynamics (SMD) of leucine unbinding in $LeuT_{Aa}$[36] and based on the several crystal structures of $LeuT_{Aa}$ containing ligands within the S2 site.[21,34–37] Additionally we demonstrate that it is possible to position 3-substituted imipramine analogs that do indeed fit into a hSERT homology model occupying both the S1 and the S2 site. The biological studies performed on wt hSERT and selected mutants revealed that the shortest linkers yielded the most potent inhibitors, and that they most likely are occupying the S1 and S2 sites simultaneously.

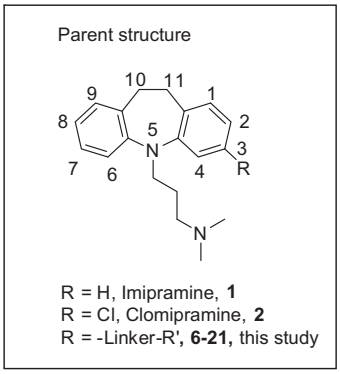

Figure 1. Structure of imipramine, clomipramine and the imipramine analogs **6–21** of this study.

2. Results

2.1. Steered MD

Similar to what has previously been explored for leucine (un) binding in $LeuT_{Aa}$[36] we performed Steered Molecular Dynamics (SMD) simulations of the unbinding of imipramine from the central S1 site of hSERT initiated from the previously biochemically validated binding mode.[9] This methodology has proven useful in exploring the relative stability of binding sites within a binding event. Based on two 25 ns SMD simulations of imipramine from the central S1 binding site of a dimer hSERT to the extracellular space we were able to identify at least one secondary transient binding site. In all four hSERT monomers we identified a secondary binding site within the extracellular vestibule approximately 10–12 Å above the central S1 site (Fig. 2). This site corresponds to the site previously described to bind several compounds within $LeuT_{Aa}$[21,38–40] and which has also been identified from SMD simulations of $LeuT_{Aa}$.[36,38] From this secondary binding site we could get an estimate of the binding distance between two imipramine molecules (Fig. 2). Based on the predicted favorable binding sites of imipramine we estimated an advantageous distance between the two imipramine molecules to be ~10 Å, and based on this we designed novel molecular fragments that could possible occupy both binding sites simultaneously, thereby possessing improved binding affinity over a single imipramine alone. Previously, we also observed that imipramine docked into the S2 site was orientated with the alkyl amine pointing towards the central S1 binding site.[9]

2.2. Induced fit docking

Several antidepressants have been shown to also possess allosteric properties,[39,40] and it has been suggested that they exert their effect by binding to a vestibular site located above the S1 site.[20] We hypothesized that a ligand utilizing both sites with a linker of the appropriate length could have improved potency and selectivity. As no details exist about the possible orientation of a antidepressant analog in S2 we chose a linker with high flexibility. To test our hypothesis we conceived a series of imipramine based ligands consisting of an imipramine moiety attached via a linker to a naphthyl or iminodibenzyl fragment (Figs. 1 and 4). We chose the iminodibenzyl moiety because it is found in tricyclic antidepressants, which bind to the S1 in hSERT[9] and may also have affinity for the putative S2 site in hSERT based on the affinity of TCAs for S2 in LeuT.[21] However, the putative S2 site in hSERT may also be considerably smaller than in LeuT because LeuT L29, believed to line the S2 site, corresponds to the much larger W103 in hSERT. To compensate for the possibility of a smaller S2 site in hSERT we also chose the aromatic naphthyl moiety instead of iminodibenzyl for a series of the bifunctional inhibitors.

Induced fit docking calculations were performed for two of these novel compounds, **8** and **12** (Fig. 4), to explore their binding to hSERT. We chose these two compounds to isolate and explore the effect of linker length in docking simulations. No poses were obtained from the docking of compound **12**, probably due to the relatively long linker, which might accommodate greater

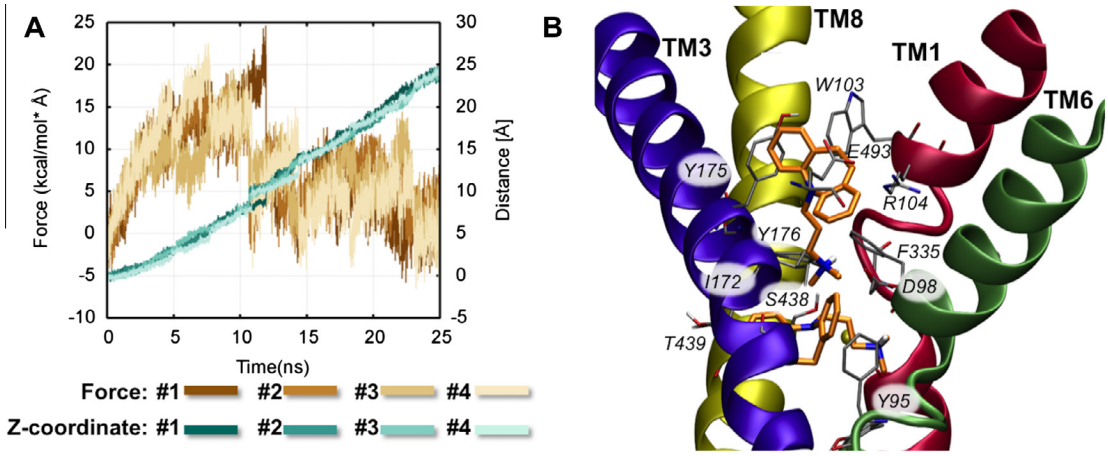

Figure 2. (A) Force profile (brown colors) and *z*-coordinate (green colors) during steered molecular dynamics as a function of time. Build-up in force indicates a favorable interaction site. In all simulations the S1 site ($z = 0$) is the most favorable site and at least one second transient site is observed approximately 10 Å above the S1 site similar to the previously described S2 site. (B) Position of imipramine (orange) in the initial S1 site and the proposed next stable S2 site obtained from the SMD calculations.

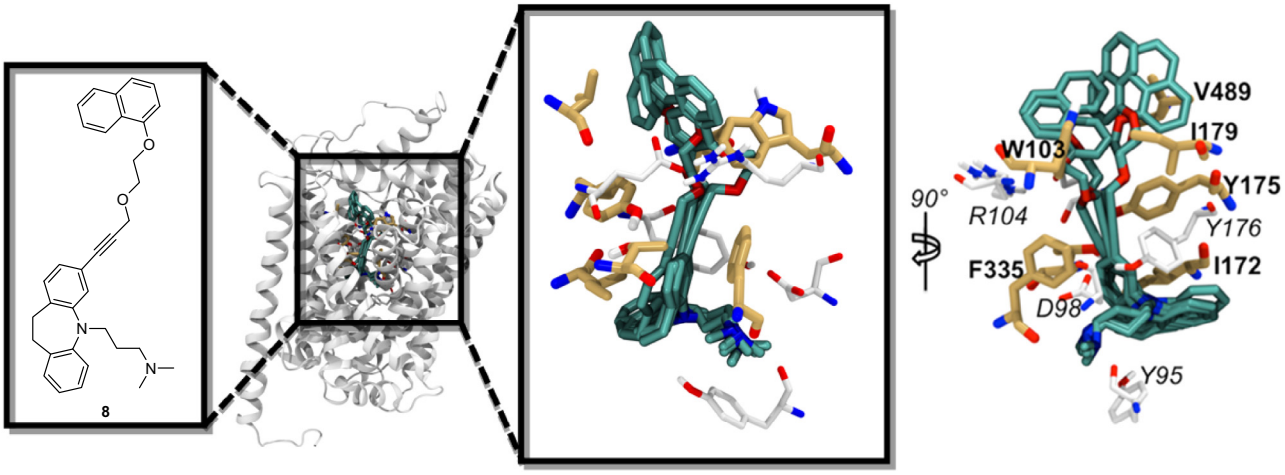

Figure 3. All four poses of compound **8** (green) within hSERT. Residues mutated in this study are shown in fat light brown sticks while selected residues are shown in gray sticks. Only residue positions from the highest scoring pose are shown. The position of the binding site is shown on the left and zoom in on the binding site in two different orientations are shown in the middle and to the right.

conformational changes within the protein. We were however able to dock **8** and the binding mode of the imipramine moiety strongly resembles the binding mode previously validated.[9] Four poses were obtained from the docking calculations and the binding with the position of the naphthyl-group varying the most between them. All four binding modes can be seen in Figure 3. The naphthyl-group of **8** is located in the S2 site similar to what was observed from the steered MD simulations, placing this group in close proximity to the salt bridge (Arg104-Glu493) within the extracellular vestibule. The average GScore from the docking calculations is −15.5 kcal/mol. It is evident that the 3-linked molecules are able to occupy both the S1 and S2 sites simultaneously in induced fit docking calculations.

2.3. Organic synthesis

Based on the promising results from the computational studies we set out to synthesize a series of imipramine ligands to be explored in biological test with hSERT and validate the computational results. According to our imipramine binding model[9,37] it was decided to attach the linker to the 3-position of one of the benzo-moieties resulting in the general ligand design shown in Figure 1, **6**–**21**.

We speculated whether it would be possible to use the chlorine atom of the easily obtainable pharmaceutical drug clomipramine (**2**) as a chemical handle for attachment of the linker through a Sonogashira coupling reaction with the linker functionalized with a terminal alkyne. In literature, most examples of Sonogashira couplings with chlorides utilize simple, activated aryl chlorides as starting material.[41,42] In comparison, clomipramine (**2**) is a functionalized aryl chloride, and accordingly only very few examples exists of similarly demanding Sonogashira couplings.[43,44] As a test system the reaction was initially explored with clomipramine **2** and propargyl alcohol (Scheme 1) using conditions inspired by work of the Buchwald group.[45,46] As no reaction took place, a second substrate investigated was the tetrahydropyran (THP)-protected propargyl alcohol, and to our delight this gave the desired Sonogashira coupled product in an acceptable yield of 63%. We were unable to improve the yield by addition of a Cu(I) co-catalyst or by altering either the base, temperature, or reaction medium.

Satisfied with this initial synthetic result we settled on a series of ligands to be prepared to validate our computational results. The structure of the linker and the R' group fragments attached to imipramine at the 3-position (Fig. 1) are shown in Figure 4. Varying lengths of ethylene glycols or β-propylene glycol were chosen as linkers to separate the imipramine fragment from the R′-group,

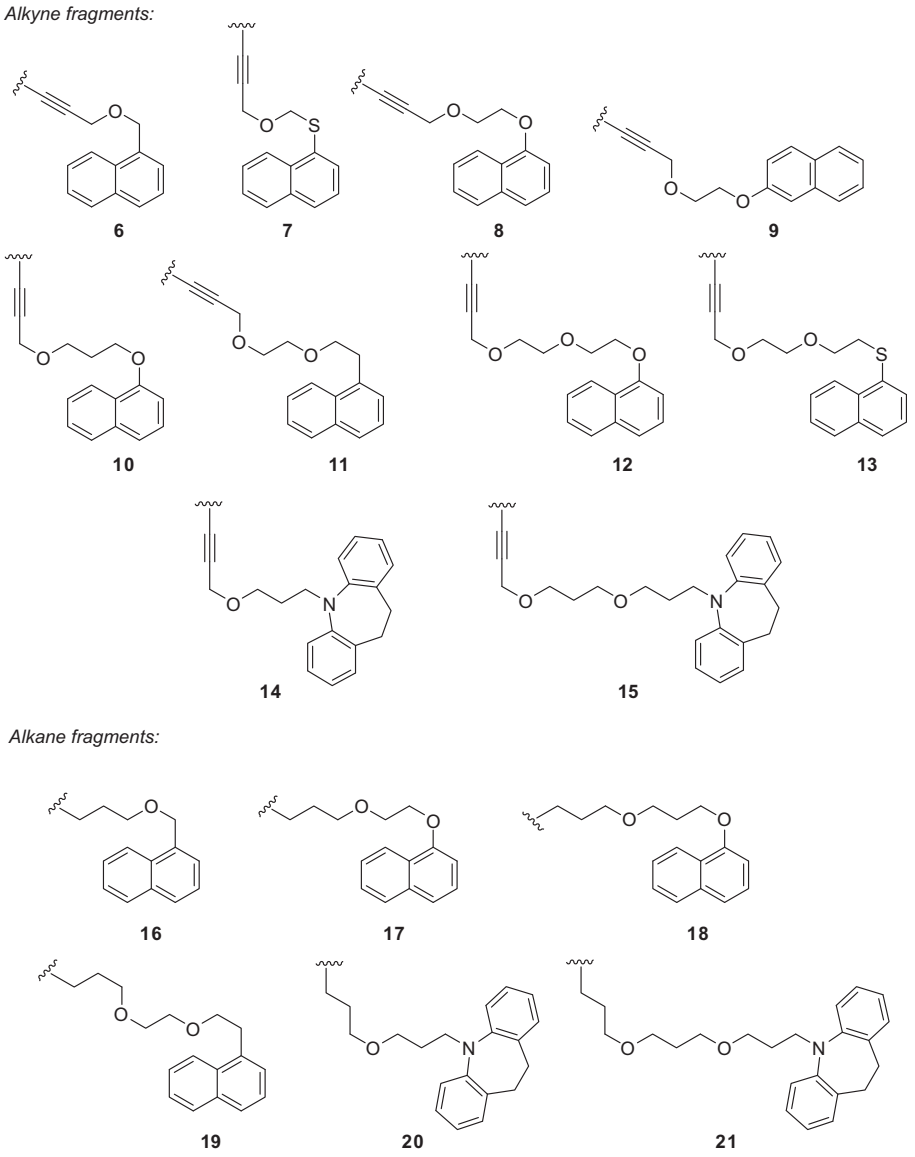

Figure 4. R group structure. Compound number refers to the whole structure, and not just the shown fragment.

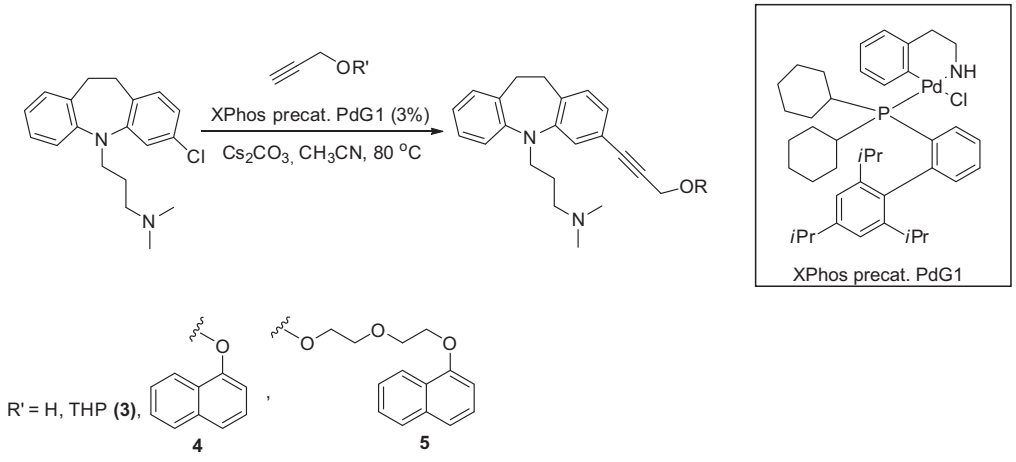

Scheme 1. Exploration of clomipramine (**2**) as a Sonogashira substrate.

(Fig. 4). As mentioned, ligands bearing both a naphthyl and the iminodibenzyl skeleton of imipramine in place of R′ were planned to be synthesized to assess the tolerance of steric bulk in the S2 site.

The proposed ligands (**6**–**15**, Fig. 4) cover all linker lengths from five to eleven atoms between the imipramine moiety and the naphthyl/iminodibenzyl R′-group. Ligands **8** and **9** allowed us to test whether there would be a difference in binding between a 1- and a 2-linked naphthyl fragment. The presence of an alkyne functionality would also allow us to easily expand our collection of ligands by simple alkyne reduction to the corresponding alkanes **16**–**21**.

We also conceived the molecules **22** and **23** (Fig. 5) to see the effect of the alkyne function itself. Simple substituents like 3-Cl or 3-CN[9] and 3,7-di-CH_3[37] have been found to lead to 2-6 fold increased inhibitory potency.

For the synthesis of the proposed ligands (**6** and **12**, Fig. 4) a convergent approach was investigated involving direct Sonogashira cross coupling on alkynes **4** and **5**. Using the exact same experimental procedure as for THP-protected propargyl alcohol failed to give the desired products **6** and **12** suggesting that THP-protected propargyl alcohol is a privileged substrate in this reaction. As a consequence of these failed reactions it was decided to carry on with a linear synthesis by deprotection and extension of the key intermediate **3**. This required the synthesis of a series of fragments that would carry a good leaving group and take part in a Williamson ether synthesis with propargyl alcohol **22** (Scheme 2). Accordingly, the THP-group was removed by treatment with excess *p*TsOH in methanol which afforded alcohol **22** in 72% yield. The ether forming reaction between this key intermediate and either an iodide or tosylate functionalized linker would then result in the first series of 3-functionalized alkyne linked imipramines (Scheme 2). A detailed description of the linker synthesis and attachment can be found in Section 5.

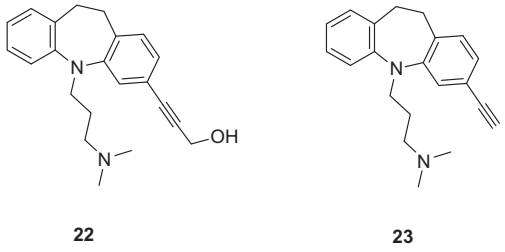

Figure 5. Structure of short 3-substituted imipramine **22** and **23**.

The reverse strategy for ether formation was also explored (not shown) where a good leaving group in the form of a mesylate was to be attached to the key intermediate **22**, and then substituted by a linker bearing an alcohol. This route, however, proved not to be feasible for obtaining **6**–**15**.

When all alkyne linked ligands **6**–**15** had been successfully synthesized, they were to be reduced to the corresponding alkane ligands by catalytic hydrogenation. This approach (Path A, Scheme 2) was only successful for the alkyne ligands **6**, **14** and **15** to give the corresponding alkane ligands in 27%, 85% and 93% yield, respectively. The remaining alkyne ligands could not be reduced by this protocol so their corresponding alkanes were prepared through reduction of propargyl alcohol **22** to the saturated analog **24**, followed by linker attachment as previously described in the alkyne series (Path B, Scheme 2). Alkynes **8**, **10**, **11**, **14** and **15** were successfully converted to alkane ligands **17**–**19** in 5%, 9%, 18% and 20% yield over two steps, respectively.

The simple ligand **23** was prepared from clomipramine in a Sonogashira reaction with (Triisopropylsilyl)acetylene. Deprotection using TBAF afforded the analog **23** as shown in Scheme 3.

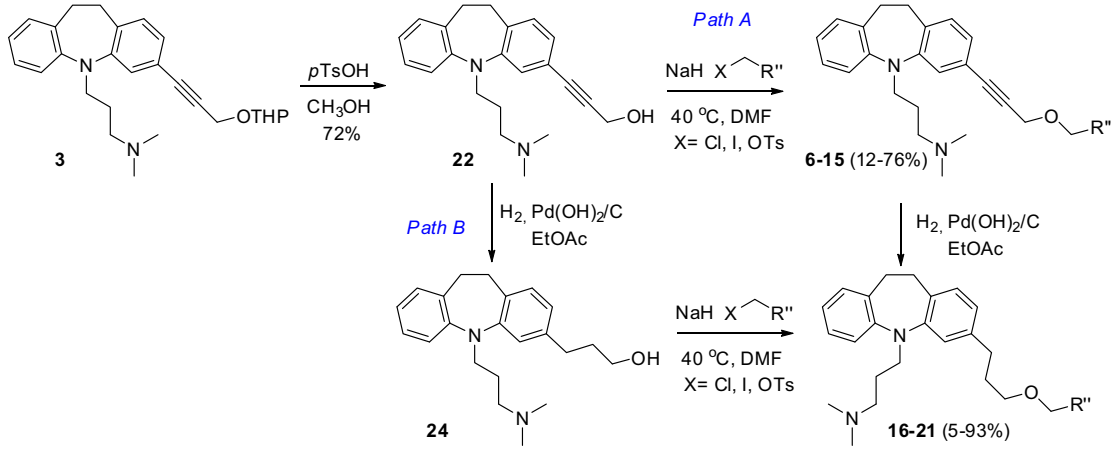

Scheme 2. Synthesis of target alkynes and alkanes through propargyl alcohol. –Linker-R′ = $CCCH_2OCH_2R''$ or $(CH_2)_3OCH_2R''$.

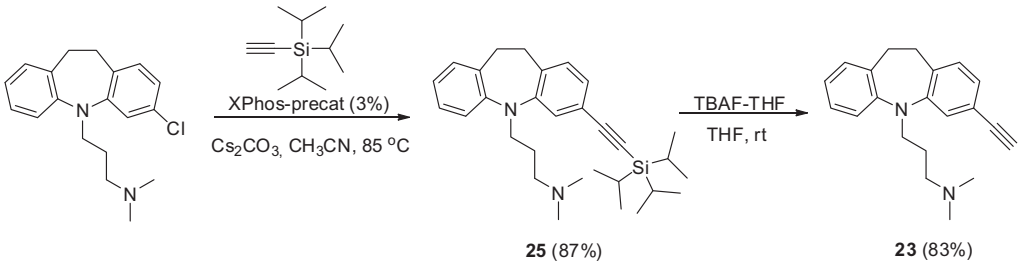

Scheme 3. Synthesis of analog **23**.

Table 1
Mean K_i values (nM) measured for inhibition of [^{3}H]-5-HT uptake by HEK-293-MSR cells transiently transfected with hSERT wt or mutants

Compound	R-group structure	Wt hSERT (nM) K_i (95%)	W103A (nM) IC_{50} (95%)	I179C (nM) K_i (95%)	I172M (nM) K_i (95%)
1	—H	31 [10;97], $n = 6$	2.6 [1.6;4.3], $n = 5$	5.7 [2.1;15], $n = 6$	1300 [890;1900], $n = 4$
6	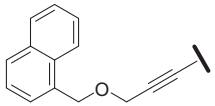	590 [290;1200], $n = 4$	340 [60;1800], $n = 4$	280 [74;1100], $n = 3$	5400 [1000;28,000], $n = 3$
7	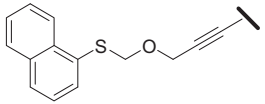	1100 [630;1900], $n = 4$	350 [140;860], $n = 4$	475 [290;790], $n = 5$	4700 [2200;10,000], $n = 4$
8	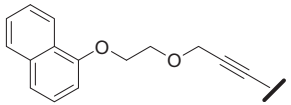	3500 [770;16,000], $n = 3$	4800 [4100;5600], $n = 3$	1800 [1000;3400], $n = 3$	8000 [1800;34,000], $n = 3$
9	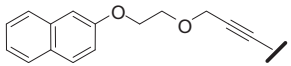	1500 [870;2600], $n = 4$	440 [110;1700], $n = 3$	640 [210;1900], $n = 4$	2000 [840;4600], $n = 4$
10	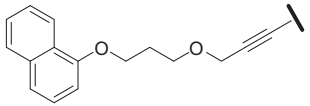	3500 [1500;8200], $n = 4$	940 [330;2700], $n = 3$	1200 [340;4200], $n = 4$	27,000 [14,000;53,000], $n = 4$
11	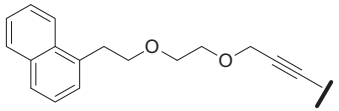	1100 [490;2600], $n = 4$	300 [230;390], $n = 4$	540 [260;110], $n = 3$	5200 [3300;8400], $n = 4$
12	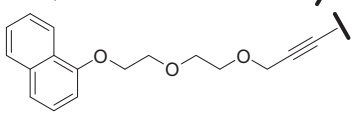	6500 [1700;25,000], $n = 3$	420 [180;1000], $n = 3$	450 [220;900], $n = 3$	6400 [1300;31,000], $n = 3$
13	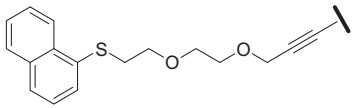	2000 [960;4300], $n = 3$	560 [450;680], $n = 4$	500 [280;900], $n = 4$	19,000 [7000;50,000], $n = 3$
14	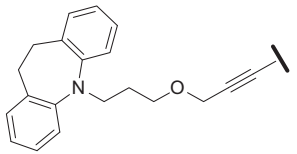	13,000 [6800;24,000], $n = 3$	1600 [370;6600], $n = 3$	1600 [240;10,000], $n = 3$	16,000 [3800;65,000], $n = 3$
15	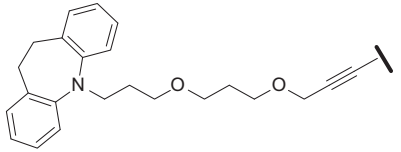	11,000 [6800;17,000], $n = 3$	4100 [1400;12,000], $n = 4$	2800 [1500;5200], $n = 4$	10,000 [4000;26,000], $n = 4$
16	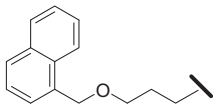	620 [170;2300], $n = 3$	610 [280;1300], $n = 4$	290 [120;670], $n = 3$	5000 [1200;22,000], $n = 3$

17	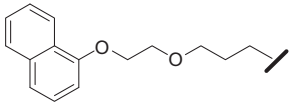	600 [220;1700], $n = 3$	280 [90;860], $n = 3$	270 [130;550], $n = 3$	2700 [2100;3500], $n = 4$
18	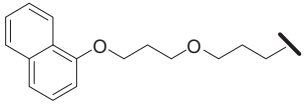	1200 [630;1900], $n = 5$	600 [190;1900], $n = 5$	620 [250;1500], $n = 5$	9400 [4400;20,000], $n = 5$
19	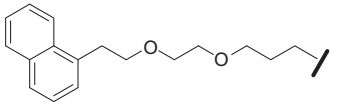	1000 [650;1700], $n = 4$	280 [90;890], $n = 3$	360 [250;500], $n = 4$	6700 [2900;15,000], $n = 5$
20	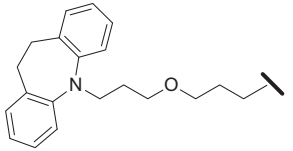	6300 [2400;16,000], $n = 3$	270 [150;480], $n = 3$	330 [90;1200], $n = 3$	15000 [6100;68,000], $n = 3$
21	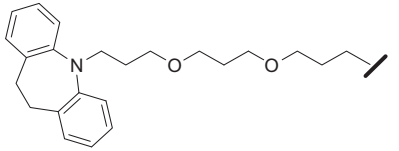	5900 [3000;12,000], $n = 3$	840 [330;2300], $n = 3$	640 [150;2700], $n = 3$	11000 [1500;86,000], $n = 3$
22	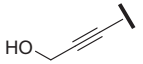	150 [50;420], $n = 3$	60 [20;170], $n = 3$	35 [24;52], $n = 4$	2600 [1400;4900], $n = 5$
23		220 [110;460], $n = 4$	40 [8;160], $n = 3$	27 [12;63], $n = 3$	2400 [1200;4900], $n = 4$

W103A was not active enough to yield a K_M, making conversion of W103A IC_{50} to K_i impossible. For this mutant we report an IC_{50}. 95% confidence limits are shown in brackets.

With the series of target molecules in hand, covering different chain lengths, and being a collection of 12 alkyne and 6 alkane ligands, we set out to investigate their ability to inhibit hSERT.

2.4. Inhibitory potencies of novel dimeric inhibitors for hSERT S1 and S2 site mutants

The aim of the biochemical experiments was to evaluate the inhibitory potency of the bi-functional ligands in a SAR-study by uptake inhibition experiments on wt hSERT. Secondly, we wanted to use selected mutants located in the S1 and S2 site to reveal whether the ligands occupy the S1 and/or S2 site to qualify whether a utilization of both sites had positive effects on potency and would be a desirable strategy for inhibitor design. Inhibitory potencies are shown in Table 1. As seen in Figure 3, W103 and I179 are located in the putative S2 that would be occupied by the 3-linked moiety of the compounds if they utilized both sites, while I172 is located within the central S1 binding site. The location of I172 in the central substrate site (later coined S1) was established by Rudnick and co-workers many years prior to the first structural insights.[47] Blakely and co-workers have demonstrated a key role of this residue in coordinating high affinity inhibitors[48] and proceeded to establish an antidepressant-insensitive knock-in hSERT I172M mouse.[49] By determining the orientation of an SSRI[11] and a TCA in the S1 site[9] we have previously been able to show how I172 was nested into the curved heteroaromatic substructure of imipramine, readily explaining the detrimental effects of the I172M mutation on imipramine potency and suggesting how the sensitivity to the I172M mutation could be a marker of S1 site utilization by a ligand. Large bi-functional inhibitors, as in the current study, might in some instances not reach the S1 and therefore we used the sensitivity to I172M as a marker for S1 site binding.

2.5. Inhibitory potencies of 3-linked imipramine analogs for inhibition of the human serotonin transporter

In an initial SAR analysis we were interested in whether the introduced substitutions affected analog potency relative to the parent compound, imipramine. Overall, we found that all the studied analogs exhibited significantly decreased potency for inhibition of hSERT wt relative to imipramine (p <0.05, one-way ANOVA, Dunnett's post hoc test).

The ligands **22** and **23** (Table 1) with small 3-substituents show that the presence of an alkyne function itself at this position significantly decreases binding to wt hSERT as opposed to other small substituents like 3-Cl and 3-CN which have earlier been found to increase potency.[9] Increasing the size of the 3-substituent by going to bi-functional ligands with the shortest alkyne linker results in further lowering of inhibitory potency, i.e., the potency of **6** is significantly decreased relative to **23**. The slightly longer alkane linker of **16** yields a very similar potency as **6** and is also significantly decreased relative to **24**, which is the most relevant reference compound. These were, together with alkane **17**, however the most potent of the bi-functional ligands. The naphthyl displaying ligands having longer linkers are generally worse inhibitors of wt hSERT.

The optimal point of attachment of the linker to the naphthyl group is most directly assessed by the comparison of the 2-naphthyl displaying ligand **9** and the 1-naphthyl displaying ligand **8**, which have identical linker length and linker chemistry. Although the 2-substituted **9** appears to have higher potency than **8**, this falls short of statistical significance.

We utilized two different classes of substituents at the end of the linker. Viewed as a group, the larger iminodibenzyl containing ligands **14**, **15**, **20**, **21** (group mean = 8500 nM), were found to be significantly less potent against wt hSERT than the naphthyl containing ligands **6**–**13** and **16**–**19** (group mean = 1510 nM) when compared as two groups (p <0.0001, two-tailed t-test). They inhibit wt hSERT to the same extent as we previously observed for nitrogen interlinked imipramine dimers (Fig. 6).[50]

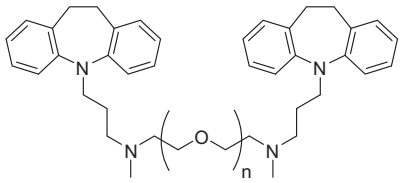

n= 1, (IC_{50} 6000 nM) 2, (IC_{50} 4800 nM) 3 (IC_{50} 5500 nM)

Figure 6. Inhibitory potency of nitrogen interlinked imipramine dimers.

Modification of the ligand may alter the preference for binding sites, i.e., where imipramine prefers the S1 site, a bivalent imipramine analog may now prefer both the S1 and S2 sites or it may only prefer S2. We have included three mutants in the study to enable such classification, one in S1 and two in the larger and more versatile S2. The effect of these mutations on inhibitor potency relative to hSERT wt will aid us in determining which sites are utilized by the ligands.

Trp103 is a sterically demanding residue located within the proposed S2 site. When mutating this residue to the much smaller alanine, we do however also see a positive effect on the potency of almost all the 3-coupled ligands. The larger ligands do obtain a relative larger gain in affinity and for example ligand **14** obtains an 8-fold increase in affinity (p = 0.004, two-tailed t-test), while molecule **20** obtains a 23-fold increase in affinity (p = 0.0002, two-tailed t-test). The only molecule out of the 20 compounds not showing a large increase in potency upon the W103A mutation is compound **8**, which could possibly be caused by favorable aromatic interactions between the naphthyl moiety and W103 as seen for the docking poses (Fig. 3).

The residue Ile179 is considered to be located in the proposed S2 site, thus mutation of this to the smaller Cys will increase the size of the S2 binding pocket and likely also the funnel connecting S1 and S2. Interestingly, the ligands containing the iminodibenzyl fragments (**14**, **15**, **20** and **21**) were affected positively by the I179C mutation, becoming significantly more potent (hSERT wt group mean = 8500 nM vs hSERT I179C group mean = 1060 nM, p = 0.0084).

Ile172 is positioned within the central S1 binding site and mutation of this residue into methionine decreased the potency for almost all molecules (hSERT wt group mean = 2100 nM vs hSERT I179C group mean = 7100 nM, p <0.0001). The fact that almost all ligands are affected by the S1 single point mutation indicates that almost all molecules are occupying the central binding pocket forming favorable interactions with Ile172 (Fig. 3), which accordingly are destroyed by the I172M mutation.[52] The loss of affinity can potentially be due to steric clashes introduced by the slightly longer methionine side chain than seen in wt and/or loss of hydrophobic interactions between Ile and imipramine within the wt protein. However, a group of structurally diverse bivalent ligands (compounds **9**, **12**, **14**, **15**) show little or no loss of affinity in the I172M mutant relative to wt hSERT which could be a sign that these ligands do either not utilize the S1 site for binding or that they do so in a different orientation than imipramine.

3. Conclusions

The computer simulations clearly illustrate the presence of a transient S2 site in hSERT at a position previously described within

LeuT[21,36,38–40,42] however, with a lower affinity than observed for the central binding site as judged from the SMD simulations. Based on the spatial organization between the S1 and S2 site we were able to construct 3-linked imipramine analogs which were additionally tested through molecular docking, clearly illustrating that these bi-functional ligands are able to occupy the central and extracellular binding sites simultaneously. Based on these results the synthesis of 3-linked imipramine ligands to be used for biological studies of hSERT, was undertaken. In total 19 ligands were synthesized using a copper-free Sonogashira reaction as the key step and the drug clomipramine as the starting material. This is the first example of the Sonogashira reaction being used to directly modify a known drug, providing easy access to analogs hereof. The pharmacological data shows that the shortest alkyne ligand **6** was the most potent bi-functional ligand against wt hSERT. When the ligands were tested against W103A and I179C mutants, enlarging the S2 binding site, it was found that the larger ligands were affected positively, and to a larger extent than the smaller ligands, suggesting that the ligands are occupying the proposed S2 site, as also predicted from the computational studies. Additionally, the I172M mutation within the central binding pocket negatively affected almost all of the tested molecules which indicated that almost all the novel molecules are indeed occupying both the central S1 and the extracellular S2 site simultaneously.

The S2 site could be envisaged to have both positive and negative effects on ligand affinity depending on the ligand. If the S2 site serves as a transient vestibular binding site *en route* to S1 it would increase the local concentration of ligand experienced by the S1 site and increase association rates which in turn would increase potency. If the S2 site contributes negatively by impeding access to S1 then we would expect that enlarging the S2 site would lead to increased imipramine potency. We do indeed observe that expanding the S2 site with the W103A and I179C mutations does increase imipramine potency suggesting that the S2 site contributes negatively to imipramine potency.

Taken together, our findings serve as the starting point for design and development of a new generation of improved antidepressants that fully exploit both binding sites, and hence, possibly can achieve a better inhibitory potency than the mono-functional counterpart and possibly achieve an inhibitor that is non-competitive with 5-HT through additional use of the S2. The level of inhibition obtained with the ligands described in this article could possibly be greatly improved by exchanging the naphthyl fragment with another moiety that contributes more to binding.

4. Methods

4.1. Homology modeling

The hSERT model utilized in the study is the one previously published.[11,15,17] In summary, this model was constructed utilizing MODELLER 9v4[51,52] based on the structure of $LeuT_{Aa}$[6] utilizing the alignment by Beuming et al.[53] including extensive optimization of EL2 along with two sodium ions and one chloride ion placed as described previously.[54]

4.2. Simulation system building

The structure used for the steered molecular dynamics simulations was hSERT with imipramine bound in the same orientation as biochemically validated[9] and later confirmed from crystal structures.[18,19] The steered molecular dynamics simulations were set up in a similar way as for the SMD simulations of the (un)binding events of leucine from $LeuT_{Aa}$ (PDB 2A65) by Celik et al.[36] A dimer of hSERT with imipramine bound was constructed based on the dimer structure of $LeuT_{Aa}$.[6] The dimer was manually embedded into a pre-equilibrated POPC membrane bilayer. The system was solvated and neutralized to a 0.2 M ion concentration using NaCl.

4.3. Simulations details

The simulations were performed utilizing the NAMD program[55,56] applying the CHARMM22 force field for protein[57] and lipids including the CMAP corrections.[58] The same parameters for imipramine as previously described by Sinning et al. were used.[9] Particle Mesh Ewald[59] was used for long range electrostatic and the cutoff for the van der Waals interactions was 12 Å with a switching function applied from 10 Å. Constant pressure at 1 atm was maintained utilizing the Langevin piston method[60] with a decay time of 50 fs and an oscillation period of 100 fs. The temperature was held constant at 310 K by Langevin damping with a damping coefficient of 0.5 f s^{-1}.

In pulling simulations, a moving constraint is applied to the center of mass (COM) of a group of atoms. The chosen group of atoms will thus be forced to generally move along a specified direction while still being able to move freely along all other degrees of freedom. Constant velocity SMD was accomplished by the *tclforces* in NAMD.[60,61] The ligand SMD simulations were performed as previously described[62] with a pulling force of 500 pN/$Å^2$ and with a pulling velocity of 1 Å/ns.

4.4. Imipramine docking

Ligand **8** and **12** (Fig. 4) were docked into the combined S1 and S2 binding sites of the protein utilizing induced fit docking protocol (IFD[63]) which utilizes Glide from the Schrödinger suite[64] as previously done by us.[9,12–14,16,17,58] In short, the binding site was defined around Ile172 and Asp98. The number of poses to save was set to 100 in both initial and re-docking stage. The XP-scoring function[65] was used in the redocking stage.

4.5. Mutagenesis

The cDNA for the human serotonin transporter (Uniprot P31645) in the pCDNA 3.1 vector was used as template for the mutagenesis. Mutations were introduced by PCR using the Phusion High-Fidelity DNA polymerase (Finnzymes) and primer pairs with appropriate nucleotide mismatches followed by DpnI digestion of the parent DNA. *Escherichia coli* XL10 (Stratagene) were transformed with the mutated DNA and used for DNA production. Mutant constructs were sequenced across the entire reading frame using BigDye v3.1 chemistry (Applied Biosystems) analyzed on an ABI 3100 Sequencer (Applied Biosystems) to ensure that the transporter gene contained the desired mutations and that no unwanted mutations had been introduced.

4.6. Cell culture

Human embryonic kidney 293MSR cells (Invitrogen) were cultured in Dulbecco's modified Eagle's medium (BioWhitaker) supplemented with 10% fetal calf serum (Invitrogen), 100 U/ml penicillin, 100 μg/mL streptomycin (BioWhitaker), and 6 μg/mL Geneticin (Invitrogen) at 95% humidity and 5% p(CO_2) at 37 °C. Two days prior to the uptake assay, cells were detached by Versene (Invitrogen) and trypsin/EDTA (BioWhitaker) treatment and mixed with a preformed complex of 0.2 μg transporter DNA and 0.5 μL Lipofectamine 2000 per square centimeter of plating area (Invitrogen). The transfection mix was dispensed into white 96-well microplates (Nalgene Nunc International) at a cell density of 50–70% confluence and incubated for 48–60 h.

4.7. Uptake inhibition assay

Adherent transfected cells were washed with phosphate-buffered saline supplemented with calcium and magnesium (PBSCM: 137 mM NaCl, 2.7 mM KCl, 10 mM $Na_2HPO_4{*}H_2O$, 1.4 mM KH_2PO_4, 0.1 mM $CaCl_2$, and 1 mM $MgCl_2$, pH 7.4) and immediately preincubated for 30 min with a dilution series of the drug. Initiation of uptake was performed by adding a mix of 50–100 nM [^{3}H] 5-HT and the inhibitor in the same concentration as in the preincubation. This incubation lasted for 10 min at room temperature and was terminated by aspiration and washing with PBSCM. The amount of accumulated radioactive neurotransmitter was determined by lysing the cells with Microscint 20 (PerkinElmer) and quantified on a Packard Topcounter.

4.8. Data analysis

Analysis of all data was carried out in GraphPad Prism 5.0 software (GraphPad Inc., San Diego, CA). Radioactive counts from [^{3}H] 5-HT were fitted by sigmoidal dose–response curve for determination of IC_{50}-values. The IC_{50}-values were converted to K_i-values using the Cheng–Prusoff equation.[66]

One-way ANOVA with Dunnett's post hoc test and the Student *t*-test was used for statistical comparison of K_i values.

5. Experimental

5.1. General methods

Moisture sensitive reactions were carried out in oven (ca. 120 °C) or flame dried glassware, under a N_2 or Ar atm, in solvents dried according to standard procedures. TLC analysis was performed on aluminum sheets coated with silica gel (Merck kiesel, 60, F254) and were visualized by either UV-irradiation or staining with a $KMnO_4$ ($KMnO_4$ and NaOH in H_2O) or Cmol ($(NH_4)_6Mo_7O_{24}{\cdot}4H_2O$, $Ce(SO_4)_2$ and H_2SO_4 in H_2O) solution, and heated until spots appeared. Flash column chromatography was performed using Merck silica 60 (230–400 mesh) as stationary phase.^{1}H NMR, and ^{13}C NMR were recorded on a Varian Mercury 400 spectrometer, at 400 MHz, and 100 MHz respectively. Mass spectral data were recorded on a Micromass LC-TOF instrument as electrospray experiments. Melting points were measured on a Büchi B-450, and are not corrected.

5.1.1. General procedure A: Coupling procedure to the formation of ligands 6, 8, 12–15

The alcohol **22** (1 equiv) was dissolved in anhydrous DMF to a concentration of 0.37 mol/L, under a N_2 atm, before NaH (60%, 2 equiv) and the appropriate iodide or tosylate in case of **6** (1.3 equiv) were added. The reaction mixture was heated to 40 °C and left overnight. When the reaction had run to completion, it was quenched with H_2O and diluted with saturated $NaHCO_3$ (aq). The aqueous phase was extracted with ethyl acetate and washed alternately with H_2O and saturated $NaHCO_3$ (aq). The organic phase was dried over $MgSO_4$, filtered and evaporated. The product was purified by column chromatography.

5.1.2. General procedure B: Coupling procedure to the formation of ligands 9–11

The alcohol **22** (1 equiv) was dissolved in anhydrous DMF to a concentration of 1.9 mol/L, under a N_2 atm, before NaH (60%, 2 equiv) and the appropriate iodide (3 equiv) were added to the solution. The reaction mixture was heated to 40 °C. When the reaction had run to completion (approx. 3 h), it was quenched with H_2O and diluted with saturated $NaHCO_3$ (aq). The aqueous phase was extracted with AcOEt and washed alternately with H_2O and saturated $NaHCO_3$ (aq). The organic phase was dried over $MgSO_4$, filtered and evaporated. The product was purified by column chromatography.

5.1.3. General procedure C: Coupling procedure to the formation ligands 17–19

The alcohol **22** (1 equiv) was dissolved in anhydrous DMF to a concentration of 1.9 mol/L under a N_2 atm. before NaH (60%, 2 equiv) and the appropriate iodide (1.5 equiv) were added. The reaction mixture was heated to 40 °C. When the reaction had run to completion (app. 3 h), it was quenched with H_2O and diluted with saturated $NaHCO_3$ (aq). The aqueous phase was extracted with AcOEt and washed alternately with H_2O and saturated $NaHCO_3$ (aq). The organic phase was dried over $MgSO_4$, filtered and evaporated. The product was purified by column chromatography.

5.1.4. General procedure D: Catalytic hydrogenation to the formation of compounds 16, 20, 21, 24

The appropriate alkyne was dissolved in AcOEt to a concentration of 0.03 mol/L, under N_2 atm, before $Pd(OH)_2/C$ (20 mol %) was added. The flask was evacuated and backfilled with H_2 (g), and then left overnight. When crude ^{1}H NMR showed complete reduction of the alkyne to the alkane, the mixture was filtered on a Celite® column and the solvent was evaporated. In most cases there was no need for further purification.

5.1.5. *N,N*-Dimethyl-3-(3-(3-(tetrahydro-2*H*-pyran-2-yl)oxy) prop-1-yn-1-yl)-10,11-dihydro-5*H*-dibenzo[*b,f*]azepine-5-yl) propane-1-amine, 3

Clomipramine **2** (0.503 g; 1.43 mmol; 1 equiv) was mixed with Cs_2CO_3 (1.13 g; 3.57 mmol; 2.5 equiv) and XPhos precatalyst PdG1 (0.0313 g; 0.0428 mmol; 3 mol %) in a glove box. To this anhydrous acetonitrile (4 mL) was added, and the reaction mixture was left with stirring, in the glove box for 25 min before THP protected propargyl alcohol (0.501 g; 3.57 mol; 2.5 equiv) was added. The reaction vessel was sealed, removed from the glove box, and then heated to 80 °C for 20 h. After 20 h the reaction mixture was cooled to rt and quenched with saturated $NaHCO_3$ (aq). The mixture was extracted with AcOEt, and the combined organic phases were dried over $MgSO_4$, filtered and evaporated. The product was purified by column chromatography (first CH_2Cl_2/CH_3OH 50:1 then CH_2Cl_2/CH_3OH 20:1). Upon repeated column chromatography, the product was isolated as brown oil in 63% yield (0.375 g; 0.895 mmol). R_f (CH_2Cl_2/CH_3OH 20:1) 0.45. ^{1}H NMR (400 MHz, $CDCl_3$) δ_H 7.16–7.02 (m, 4H), 6.99 (s, 2H), 6.94 (dt, 1H, J = 7.3, 1.1 Hz), 4.88 (t, 1H, J = 3.4 Hz) 4.46 (q, 2H, J = 15.7 Hz), 3.93–3.81 (m, 1H), 3.77 (t, 2H, J = 6.6 Hz), 3.61–3.50 (m, 1H), 3.12 (s, 4H), 2.60 (t, 2H, J = 5.6 Hz), 2.35 (s, 6H), 1.96–1.48 (m, 8H). ^{13}C NMR (100 MHz, $CDCl_3$) δ_C 147.9, 134.9, 134.4, 130.3, 129.7, 126.7, 125.9, 123.3, 123.2, 120.7, 120.4, 96.9, 86.0, 84.4, 62.1, 57.3, 54.9, 48.5, 44.9, 32.6, 31.8, 30.4, 25.5, 19.2 ppm. HRMS (ES+): Calcd for $C_{27}H_{34}N_2O_2$-H: 419.2699; found 419.2699.

5.1.6. *N,N*-Dimethyl-3-(3-(3-(naphthalene-1-ylmethoxy)prop-1-yn-1-yl)-10,11-dihydro-5*H* dibenzo[*b,f*]azepine-5-yl)propane-1-amine, 6

The product **6** was synthesized according to general procedure A, and was purified by column chromatography (first CH_2Cl_2/CH_3OH 50:1 then CH_2Cl_2/CH_3OH 10:1). The product was obtained as yellow oil in 31% yield (0.029 g; 0.0619 mmol). R_f (CH_2Cl_2/CH_3OH 10:1) 0.54. ^{1}H NMR (400 MHz, $CDCl_3$) δ_H 8.23 (d, 1H, J = 8.1 Hz), 7.86 (dd, 2H. J = 15.4, 8.1 Hz), 7.61–7.39 (m, 4H), 7.22 (s, 1H), 7.18–7.06 (m, 3H), 7.04 (s, 2H), 6.96 (dd, 1H, J = 16.1, 9.0 Hz), 5.14 (s, 2H), 4.45 (s, 2H), 3.77 (t, 2H, J = 6.9 Hz), 3.16 (s, 4H), 2.32 (t, 2H, J = 7.2 Hz), 2.16 (s, 6H), 1.73 (quint, 2H, J = 6.8 Hz). ^{13}C

NMR (100 MHz, $CDCl_3$) δ_C 148.2, 134.9, 134.6, 133.9, 133.1, 132.0, 130.3, 129.6, 129.0, 128.6, 127.3, 126.7, 126.5, 125.9, 125.6, 125.3, 124.3, 123.3, 123.1, 120.6, 120.5, 87.0, 84.3, 70.1, 58.1, 57.7, 48.9, 45.6, 32.7, 31.8, 26.2 ppm. HRMS (ES+): Calcd for $C_{33}H_{34}N_2OH$: 475.2749; found 475.2791.

5.1.7. *N,N*-Dimethyl-3-(3-(3-((naphthalene-1-ylthio)methoxy) prop-1-yn-1-yl)-10,11-dihydro-5*H*-dibenzo[*b,f*]azepine-5-yl) propane-1-amine, 7

DBU (0.570 g; 3.70 mmol; 1.2 equiv) was added to a solution of 1-thionaphthalene (0.500 g; 3.12 mmol; 1 equiv) dissolved in anhydrous CH_2Cl_2 (27 mL) under a N_2 atmosphere, and left overnight. When the reaction had run to completion the organic phase was washed with 1 M HCl and brine. The product (chloromethyl) (naphthalene-1-yl)sulfane (0.032 g; 0.151 mmol; 1 equiv), still dissolved in CH_2Cl_2, was then added to a solution of alcohol **22** (0.051 g; 0.151 mmol; 1 equiv) dissolved in anhydrous DMF (0.2 mL). CH_2Cl_2 was then evaporated and NaI (0.023 g; 0.151 mmol; 1 equiv) and NaH (0.012 g; 0.303 mmol; 2 equiv) were added to the reaction mixture. After 3 h the reaction had run to completion, and was quenched carefully with H_2O. The aqueous phase was diluted with saturated $NaHCO_3$ (aq) and extracted with AcOEt. The combined organic phases were dried over $MgSO_4$, filtered and evaporated. The product was purified by column chromatography (CH_2Cl_2/CH_3OH 50:1.5) and isolated as yellow oil in 27% yield (0.021 g; 0.0407 mmol). R_f (CH_2Cl_2/CH_3OH 10:1) 0.48. ^1H NMR (400 MHz, $CDCl_3$) δ_H 8.42 (d, 1H, J = 8.4 Hz), 7.85 (dd, 2H, J = 7.3, 4.7 Hz), 7.78 (d, 1H, J = 8.2 Hz), 7.62–7.47 (m, 2H), 7.44 (t, 1H, J = 8.0 Hz), 7.18–7.05 (m, 4H), 7.05–6.89 (m, 3H), 5.26 (s, 2H), 4.63 (s, 2H), 3.75 (t, 2H, J = 6.9 Hz), 3.15 (s, 4H), 2.33 (t, 2H, J = 7.2 Hz), 2.18 (s, 6H), 1.73 (quint, 2H, J = 7.2 Hz). ^{13}C NMR (100 MHz, $CDCl_3$) δ_C 148.1, 134.9, 134.7, 134.1, 133.3, 132.7, 130.3, 129.8, 129.6, 128.7, 128.1, 126.7, 126.6, 126.3, 125.9, 125.8, 125.2, 123.3, 123.2, 120.5, 120.3, 87.2, 83.2, 74.4, 57.6, 55.9, 48.8, 45.4, 32.7, 31.8, 25.9 ppm. HRMS (ES+): Calcd for $C_{33}H_{34}N_2OSH$: 507.2407; found: 507.2468.

5.1.8. *N,N*-Dimethyl-3-(3-(3-((naphthalene-1-yloxy)ethoxy) prop-1-yn-1-yl)-10,11-dihydro-5*H*-dibenzo[*b,f*]azepine-5-yl) propane-1-amine, 8

The product **8** was synthesized according to general procedure A, and was purified by column chromatography (first CH_2Cl_2/CH_3OH 50:1 then CH_2Cl_2/CH_3OH 10:1). The product was obtained as reddish/brown oil in 24% yield (0.034 g; 0.0709 mmol). R_f (CH_2Cl_2/CH_3OH 10:1) 0.53. ^1H NMR (400 MHz, $CDCl_3$) δ_H 8.33 (dd, 1H, J = 8.2, 1.5 Hz), 7.79 (dd, 1H, J = 7.4, 1.4 Hz), 7.52–7.32 (m, 4H), 7.22–6.90 (m, 7H), 6.84 (d, 1H, J = 7.5 Hz), 4.56 (s, 2H), 4.37 (dd, 2H, J = 5.5, 4.2 Hz), 4.12 (dd, 2H, J = 5.2, 4.5 Hz), 3.74 (t, 2H, J = 6.9 Hz), 3.15 (s, 4H), 2.29 (t, 2H, J = 6.8 Hz), 2.15 (s, 6H), 1.71 (quint, 2H, J = 7.2 Hz). ^{13}C NMR (100 MHz, $CDCl_3$) δ_C 154.7, 148.2, 134.6, 130.3, 129.6, 127.5, 126.6, 126.5, 125.9, 125.7, 125.3, 123.3, 123.1, 122.3, 120.6, 120.5, 105.0, 87.0, 84.1, 68.4, 67.9, 59.6, 57.7, 48.9, 45.6, 32.7, 31.8, 26.2. HRMS (ES+): Calcd for $C_{34}H_{36}N_2O_2H$: 505.2855; found 505.2853.

5.1.9. *N,N*-Dimethyl-3-(3-(3-(3-(2-(naphthalene-2-yloxy)ethoxy) prop-1-yn-1-yl)-10,11-dihydro-5*H*-dibenzo[*b,f*]azepine-5-yl) propane-1-amine, 9

The product **9** was synthesized according to general procedure B, and was purified by column chromatography (CH_2Cl_2/CH_3OH 50:1.5). The product was isolated as yellow oil in 28% yield (0.026 g; 0.0517 mmol). R_f (CH_2Cl_2/CH_3OH 10:1) 0.43. ^1H NMR (400 MHz, $CDCl_3$) δ_H 7.74 (dd, 3H, J = 17.6, 8.4 Hz), 7.43 (t, 1H, J = 7.5 Hz), 7.33 (t, 1H, J = 7.5 Hz), 7.22–7.08 (m, 6H), 7.08–6.92 (m, 3H), 4.51 (s, 2H), 4.34–4.27 (m, 2H), 4.10–3.98 (m, 2H), 3.75 (t, 2H, J = 6.6 Hz), 3.13 (s, 4H), 2.62 (t, 2H, J = 7.6 Hz), 2.34 (s, 6H), 1.89 (t, 2H, J = 7.2 Hz). ^{13}C NMR (100 MHz, $CDCl_3$) δ_C 156.8, 147.7, 147.6, 134.5, 130.4, 129.8, 129.5, 127.7, 126.9, 126.8, 126.5, 126.0, 123.8, 123.5, 123.0, 120.7, 120.4, 119.1, 106.9, 86.7, 84.3, 68.4, 67.4, 59.5, 57.0, 48.2, 44.3, 32.6, 31.7, 24.3. HRMS (ES+): Calcd for $C_{34}H_{37}N_2O_2H$: 505.2855; found 505.2853.

5.1.10. *N,N*-Dimethyl-3-(3-(3-(3-(naphthalene-1-yloxy)propoxy) prop-1-yn-1-yl)-10,11-dihydro-5*H*-dibenzo[*b,f*]azepine-5-yl) propane-1-amine, 10

The product **10** was synthesized according to general procedure B, and purified by column chromatography (CH_2Cl_2/CH_3OH 50:1). The product was obtained as yellow oil in 12% yield (0.012 g; 0.0226 mmol). R_f (CH_2Cl_2/CH_3OH 10:1) 0.50. ^1H NMR (400 MHz, $CDCl_3$) δ_H 8.27 (d, 1H, J = 8.0 Hz), 7.78 (d, 1H, J = 7.8 Hz), 7.51–7.31 (m, 4H), 7.18–7.01 (m, 4H), 7.01–6.89 (m, 3H), 6.84 (d, 1H, J = 7.4 Hz), 4.40 (s, 2H), 4.29 (t, 2H, J = 6.1 Hz), 3.88 (t, 2H, J = 6.2 Hz), 3.71 (t, 2H, J = 6.8 Hz), 3.14 (s, 4H), 2.37–2.21 (m, 4H), 2.16 (s, 6H), 1.71 (quint, 2H, J = 7.2 Hz). ^{13}C NMR (100 MHz, $CDCl_3$) δ_C 154.8, 148.1, 134.9, 134.6, 134.5, 130.2, 129.6, 127.5, 126.6, 126.4, 126.0, 125.7, 125.2, 123.2, 123.1, 122.1, 120.5, 120.2, 104.8, 86.6, 84.3, 67.0, 65.1, 59.2, 57.7, 48.8, 45.5, 32.6, 31.8, 29.8, 26.0. HRMS (ES+): Calcd for $C_{35}H_{38}N_2O_2H$: 519.3012; found 519.3015.

5.1.11. *N,N*-Dimethyl-3-(3-(3-(2-(2-(naphthalene-1-yl)ethoxy) ethoxy)prop-1-yn-1-yl)-10,11-dihydro-5*H*-dibenzo[*b,f*]azepine-5-yl)propane-1-amine, 11

The product **11** was synthesized according to general procedure B, and purified by column chromatography (CH_2Cl_2/CH_3OH 50:1). The product was obtained as yellow oil in 28% yield (0.027 g; 0.0501 mmol). R_f (CH_2Cl_2/CH_3OH 50:4) 0.55. ^1H NMR (400 MHz, $CDCl_3$) δ_H 8.07 (d, 1H, J = 8.3 Hz), 7.84 (d, 1H, J = 9.3 Hz), 7.75–7.69 (m, 1H), 7.53–7.42 (m, 2H), 7.42–7.34 (m, 2H), 7.20–7.08 (m, 3H), 7.08–6.94 (m, 4H), 4.42 (s, 2H), 3.87–3.67 (m, 8H), 3.41 (t, 2H, J = 7.6 Hz), 3.12 (s, 4H), 2.86 (dd, 2H, J = 9.2, 6.7 Hz), 2.49 (s, 6H), 2.14–1.94 (m, 2H). ^{13}C NMR (100 MHz, $CDCl_3$) δ_C 147.4, 147.2, 134.8, 134.3, 133.9, 132.2, 130.6, 129.9, 128.9, 127.1, 127.0, 126.9, 126.3, 126.1, 125.7, 125.6, 123.8, 122.8, 120.9, 120.3, 86.3, 84.8, 71.8, 70.3, 69.4, 59.4, 56.5, 47.7, 43.4, 33.4, 32.5, 31.7 22.9. HRMS (ES+): Calcd for $C_{36}H_{40}N_2O_2H$: 553.3168; found 533.3165.

5.1.12. *N,N*-Dimethyl-3-(3-(3-(2-(2-(naphthalene-1-yloxy) ethoxy)ethoxy)prop-1-yn-1-yl)-10,11-dihydro-5*H*-dibenzo[*b,f*] azepine-5-yl)propane-1-amine, 12

The product **12** was synthesized according to general procedure A, and purified by column chromatography (first CH_2Cl_2/CH_3OH 50:1 then CH_2Cl_2/CH_3OH 10:1). The product was obtained as yellow oil in 41% yield (0.068 g; 0.123 mmol). R_f (CH_2Cl_2/CH_3OH 10:1) 0.68. ^1H NMR (400 MHz, $CDCl_3$) δ_H 8.34–8.26 (m, 1H), 7.85–7.75 (m, 1H), 7.52–7.31 (m, 4H), 7.19–6.90 (m, 7H), 6.85–6.78 (m, 1H) 4.45 (s, 2H), 4.34 (t, 2H, J = 5.2 Hz), 4.04 (t, 2H, J = 5.4 Hz), 3.89–3.86 (m, 2H) 3.83–3.80 (m, 2H), 3.73 (t, 2H, J = 6.9 Hz), 3.14 (s, 4H), 2.30 (t, 2H, J = 6.8 Hz), 2.15 (s, 6H), 1.70 (quint, 2H, J = 6.8 Hz). ^{13}C NMR (100 MHz, $CDCl_3$) δ_C 154.6, 147.8, 134.8, 134.4, 130.3, 129.7, 127.5, 126.7, 126.5, 125.9, 125.3, 123.3, 123.1, 122.2, 120.7, 120.5, 120.4,105.1, 86.6, 84.4, 70.9, 69.9, 69.3, 68.0, 59.4, 57.2, 48.4, 44.7, 32.6, 31.7, 24.8. HRMS (ES +): Calcd for $C_{36}H_{40}N_2O_3H$: 549.3117; found 549.3126.

5.1.13. *N,N*-Dimethyl-3-(3-(3-(2-(2-(naphthalene-1-ylthio) ethoxy)ethoxy)prop-1-yn-1-yl)-10,11-dihydro-5*H*-dibenzo[*b,f*] azepine-5-yl)propane-1-amine, 13

The product **13** was synthesized according to general procedure A, and purified by column chromatography (first CH_2Cl_2/CH_3OH 50:1 then CH_2Cl_2/CH_3OH 10:1). The product was obtained as

orange/brown oil in 45% yield (0.048 g; 0.0841 mmol). R_f (CH_2Cl_2/CH_3OH 10:1) 0.46. ^1H NMR (400 MHz, $CDCl_3$) δ_H 8.45 (d, 1H, J = 8.3 Hz), 7.84 (d, 1H, J = 9.1 Hz), 7.74 (d, 1H, J = 8.2 Hz), 7.65 (d, 1H, J = 7.2 Hz), 7.53 (dddd, 2H, J = 20.5, 8.0, 6.8, 1.3 Hz), 7.44–7.37 (m, 1H), 7.19–6.91 (m, 7H), 4.40 (s, 2H), 3.77–3.62 (m, 8H), 3.20 (t, 2H, J = 7.0 Hz), 3.14 (s, 4H), 2.31 (t, 2H, J = 7.2 Hz), 2.16 (s, 6H), 1.71 (quint, 2H, J = 6.0 Hz). ^{13}C NMR (100 MHz, $CDCl_3$) δ_C 148.2, 134.9, 134.6, 134.1, 133.3, 133.1, 130.2, 129.6, 129.0, 128.7, 127.7, 126.6, 126.4, 125.7, 125.6, 125.3, 123.3, 123.1, 120.5, 86.8, 84.1, 70.4, 70.1, 69.2, 59.4, 57.7, 48.9, 45.6, 33.9, 32.6, 31.8, 26.2. HRMS (ES+): Calcd for $C_{36}H_{40}N_2O_2SH$: 565.2889; found 565.2903.

5.1.14. 3-(3-(3-(3-(10,11-Dihydro-5*H*-dibenzo[*b*,*f*]azepine-5-yl) propoxy)prop-1-yn-1-yl)-10,11-dihydro-5*H*-dibenzo[*b*,*f*] azepine-5-yl)-*N*,*N*-dimethylpropane-1-amine, 14

The product **14** was synthesized according to general procedure A, and purified by column chromatography (first CH_2Cl_2/CH_3OH 50:1 then CH_2Cl_2/CH_3OH 10:1). The product was obtained as yellow oil in 76% yield (0.120 g; 0.211 mmol). R_f (CH_2Cl_2/CH_3OH 10:1) 0.28. ^1H NMR (400 MHz, $CDCl_3$) δ_H 7.19–7.04 (m, 9H), 7.04–6.86 (m, 6H), 4.30 (s, 2H), 3.87 (t, 2H, J = 6.5 Hz), 3.75 (t, 2H, J = 6.6 Hz), 3.62 (t, 2H, J = 6.7 Hz), 3.14 (s, 8H), 2.31 (t, 2H, J = 6.8 Hz), 2.16 (s, 6H), 1.90 (quint, 2H, J = 6.3 Hz), 1.72 (quint, 1H, J = 6.8 Hz). ^{13}C NMR (100 MHz, $CDCl_3$) δ_C 148.4, 148.2, 134.9, 134.5, 134.4, 130.2, 129.9, 129.6, 126.6, 126.5, 125.7, 123.3, 123.0, 122.5, 120.6, 120.5, 120.1, 86.5, 84.4, 68.1, 59.0, 57.7, 48.9, 47.6, 45.7, 32.6, 32.3, 31.8, 28.3, 26.3. HRMS (ES+): Calcd for $C_{39}H_{43}N_3OH$: 570.3484; found 570.3508.

5.1.15. 3-(3-(3-(3-(3-(10,11-Dihydro-5*H*-dibenzo[*b*,*f*]azepine-5-yl)propoxy)propoxy)prop-1-yn-1-yl)-10,11-dihydro-5*H*-dibenzo [*b*,*f*]azepine-5-yl)-*N*,*N*-dimethylpropane-1-amine, 15

The product **15** was synthesized according to general procedure A, and was purified by column chromatography (first CH_2Cl_2/CH_3 OH 50:1 then CH_2Cl_2/CH_3OH 10:1). The product was obtained as light yellow oil in 40% yield (0.067 g; 0.107 mmol). R_f (CH_2Cl_2/CH_3 OH 10:1) 0.48. ^1H NMR (400 MHz, $CDCl_3$) δ_H 7.19–7.05 (m, 10H), 7.02–6.87 (m, 5H), 4.26 (s, 2H), 3.82 (t, 2H, J = 6.8 Hz), 3.74 (t, 2H, J = 6.9 Hz), 3.58 (t, 2H, J = 6.4 Hz), 3.47 (quint, 4H, J = 6.3 Hz), 3.16 (s, 8H), 2.31 (t, 2H, J = 7.2 Hz), 2.16 (s, 6H), 1.84 (m, 4H), 1.71 (quint, 2H, J = 6.4 Hz). ^{13}C NMR (100 MHz, $CDCl_3$) δ_C 148.4, 148.2, 134.9, 134.5, 134.3, 130.2, 129.9, 129.6, 126.6,126.5, 125.6, 123.3, 123.1, 122.5, 120.6, 120.5, 120.1, 86.3, 84.5, 68.7, 67.8, 67.3, 59.0, 57.7, 48.9, 47.6, 45.6, 32.6, 32.4, 31.8, 30.1, 28.4, 26.2. HRMS (ES+): Calcd for $C_{42}H_{49}N_3O_2H$: 628.3903; found 628.3958.

5.1.16. *N*,*N*-Dimethyl-3-(3-(3-(naphthalene-1-ylmethoxy) propyl)-10,11-dihydro-5*H*-dibenzo[*b*,*f*]azepine-5-yl)propane-1-amine, 16

The product **16** was hydrogenated following general procedure D, and purified by column chromatography (first CH_2Cl_2/CH_3OH 50:1 then CH_2Cl_2/CH_3OH 10:1). The product was obtained as colorless oil in 27% yield (9 mg; 0.0186 mmol). R_f (CH_2Cl_2/CH_3OH 15:1) 0.47. ^1H NMR (400 MHz, $CDCl_3$) δ_H 8.14 (d, 1H, J = 8.1 Hz), 7.85 (dd, 2H, J = 23.7, 8.8 Hz), 7.57–7.40 (m, 4H), 7.13–7.02 (m, 3H), 6.97 (d, 1H, J = 7.7 Hz), 6.93–6.87 (m, 2H), 6.69 (dd, 1H, J = 7.7, 1.6 Hz), 4.96 (s, 2H), 3.72 (t, 2H, J = 6.9 Hz), 3.58 (t, 2H, J = 6.3 Hz), 3.13 (s, 4H), 2.64 (t, 2H, J = 7.4 Hz), 2.28 (t, 2H, J = 7.0 Hz), 2.13 (s, 6H), 1.93 (quint, 2H, J = 6.4 Hz), 1.69 (quint, 2H, J = 6.0 Hz). ^{13}C NMR (100 MHz, $CDCl_3$) δ_C 148.5, 148.3, 140.2, 134.7, 134.2, 133.9, 131.9, 131.4, 129.9, 129.8, 128.6, 126.4, 126.2, 125.9, 125.4, 124.2, 122.5, 120.2, 120.1, 71.6, 69.9, 57.9, 48.9, 45.7, 32.4, 32.3, 32.1, 31.7, 26.3. HRMS (ES+): Calcd for $C_{33}H_{38}N_2OH$: 479.3062; found 479.3115.

5.1.17. *N*,*N*-Dimethyl-3-(3-(3-(2-(naphthalene-1-yloxy)ethoxy) propyl)-10,11-dihydro-5*H*-dibenzo[*b*,*f*]azepine-5-yl)propane-1-amine, 17

The product **17** was synthesized according to general procedure C, and purified by column chromatography (CH_2Cl_2/CH_3OH 50:1). The product was obtained as yellow oil in 10% yield (9 mg; 0.0169 mmol). R_f (CH_2Cl_2/CH_3OH 50:4) 0.51. ^1H NMR (400 MHz, $CDCl_3$) δ_H 8.31 (d, 1H, J = 9.6 Hz), 7.79 (d, 1H, J = 7.7 Hz), 7.52–7.31 (m, 3H), 7.12–6.80 (m, 8H), 6.74 (d, 1H, J = 9.1 Hz), 4.31 (t, 2H, J = 5.2 Hz), 3.94 (t, 2H, J = 5.2 Hz), 3.73 (t, 2H, J = 6.9 Hz), 3.62 (t, 2H, J = 6.4 Hz), 3.12 (s, 4H), 2.66 (t, 2H, J = 7.6 Hz), 2.30 (t, 2H, J = 7.2 Hz), 2.14 (s, 6H), 1.92 (t, 2H, J = 6.4 Hz), 1.70 (quint, 2H, J = 7.2 Hz). ^{13}C NMR (100 MHz, $CDCl_3$) δ_C 154.8, 148.5, 140.2, 134.7, 129.9, 129.8, 127.5, 126.5, 126.0, 125.3, 122.6, 122.3, 120.6, 120.2, 120.1, 105.1, 70.9, 69.5, 68.1, 57.8, 48.9, 45.6, 32.4, 32.2, 32.1, 31.6, 26.2. HRMS (ES+): Calcd for $C_{34}H_{40}N_2O_2H$: 509.3168; found 509.3167.

5.1.18. *N*,*N*-Dimethyl-3-(3-(3-(3-(naphthalene-1-yloxy)propoxy) propyl)-10,11-dihydro-5*H*-dibenzo[*b*,*f*]azepine-5-yl)propane-1-amine, 18

The product **18** was synthesized according to general procedure C, and purified by column chromatography (CH_2Cl_2/CH_3OH 50:1.5). The product was obtained as light yellow oil in 10% yield (0.014 g; 0.0272 mmol). R_f (CH_2Cl_2/CH_3OH 10:1) 0.51. ^1H NMR (400 MHz, $CDCl_3$) δ_H 8.29 (d, 1H, J = 9.0 Hz), 7.80 (d, 1H, J = 7.2 Hz), 7.52–7.31 (m, 4H), 7.15–6.98 (m, 3H), 6.97–6.81 (m, 4H), 6.70 (d, 1H, J = 7.6 Hz), 4.27 (t, 2H, J = 6.1 Hz), 3.72 (q, 4H, J = 7.2 Hz), 3.47 (t, 2H, J = 6.4 Hz), 3.11 (s, 4H), 2.61 (t, 2H, J = 8.0 Hz), 2.32 (t, 2H, J = 7.2 Hz), 2.27–2.11 (m, 8H), 1.88 (quint, 2H, J = 7.2 Hz), 1.72 (quint, 2H, J = 7.6 Hz). ^{13}C NMR (100 MHz, $CDCl_3$) δ_C 154.9, 148.4, 148.3, 140.2, 134.6, 131.4, 129.9, 129.8, 127.6, 126.5, 126.1, 125.2, 122.6, 122.2, 120.2, 120.1, 104.8, 70.4, 67.6, 65.2 (, 57.8 (1C, 16), 48.9, 45.5, 32.4, 32.3, 32.0, 31.6, 30.0, 26.1. HRMS (ES+): Calcd for $C_{35}H_{42}N_2O_2H$: 523.3325; found 523.3325.

5.1.19. *N*,*N*-Dimethyl-3-(3-(3-(2-(2-(naphthalene-1-yl)ethoxy) ethoxy)propyl)-10,11-dihydro-5*H*-dibenzo[*b*,*f*]azepine-5-yl) propane-1-amine, 19

The product **19** was synthesized according to general procedure C, and purified by column chromatography (CH_2Cl_2/CH_3OH 50:1.5). The product was obtained as light yellow oil in 10% yield (0.012 g; 0.0216 mmol). R_f R_f (CH_2Cl_2/CH_3OH 10:1) 0.50. ^1H NMR (400 MHz, $CDCl_3$) δ) δ_H 8.08 (d, 1H, J = 8.3 Hz), 7.85 (d, 1H, J = 7.7 Hz), 7.73 (dd, 1H, J = 6.9, 2.3 Hz), 7.49 (dt, 2H, J = 13.4, 6.7 Hz), 7.43–7.35 (m, 2H), 7.14–7.02 (m, 3H), 6.99 (d, 1H, J = 7.7 Hz), 6.95–6.86 (m, 2H), 6.75 (d, 1H, J = 7.6 Hz), 3.84 (t, 2H, J = 7.6 Hz), 3.76 (t, 2H, J = 6.8 Hz), 3.69–3.55 (m, 4H), 3.47 (t, 2H, J = 6.5 Hz), 3.41 (t, 2H, J = 7.6 Hz), 3.12 (s, 4H), 2.62 (t, 2H, J = 7.6 Hz), 2.38 (t, 2H, J = 7.6 Hz), 2.19 (s, 6H), 1.88 (quint, 2H, J = 7.2 Hz), 1.76 (quint, 2H, J = 7.2 Hz). ^{13}C NMR (100 MHz, $CDCl_3$) δ_C 148.3, 140.3, 134.9, 134.7, 134.0, 132.3, 131.4, 129.9, 128.9, 127.1, 126.9, 126.5, 126.0, 125.7, 125.6, 123.9, 122.6, 120.2, 120.0, 71.8, 70.9, 70.5, 70.3, 57.7, 48.8, 45.3, 33.5, 32.4, 32.3, 32.1, 31.4, 25.9. HRMS (ES+): Calcd for $C_{36}H_{44}N_2O_2$ H: 537.3481; found 537.3481

5.1.20. 3-(3-(3-(3-(10,11-Dihydro-5*H*-dibenzo[*b*,*f*]azepine-5-yl) propoxy)propyl)-10,11-dihydro-5*H*-dibenzo[*b*,*f*]azepine-5-yl)-*N*,*N*-dimethylpropane-1-amine, 20

The product was synthesized according to general procedure D, and isolated as yellow oil in 85% yield (0.062 g; 0.108 mmol). R_f (CH_2Cl_2/CH_3OH 15:1) 0.32. ^1H NMR (400 MHz, $CDCl_3$) δ_H 7.16–7.05 (m, 10H), 6.99–6.86 (m, 4H), 6.68 (dd, 1H, J = 7.6, 1.6 Hz), 3.85 (t, 2H, J = 6.8 Hz), 3.75 (t, 2H, J = 6.9 Hz), 3.45 (t, 2H, J = 6.2 Hz), 3.37 (t, 2H, J = 6.4 Hz), 3.21–3.08 (m, 8H), 2.55 (t, 2H, J = 7.6 Hz), 2.32 (t, 2H, J = 7.2 Hz), 2.16 (s, 6H), 1.90–1.76 (m, 4H),

1.76–1.67 (m, 2H). ^{13}C NMR (100 MHz, $CDCl_3$) δ_C 148.4, 148.3, 140.3, 134.6, 134.3, 131.4, 129.9, 129.8, 126.5, 126.4, 122.5, 120.2, 120.1, 120.0,70.3, 68.7, 57.8, 48.9, 47.8, 45.5, 32.4, 32.3, 32.0, 31.5, 28.5, 26.1. HRMS (ES+): Calcd for $C_{39}H_{47}N_3OH$: 574.3797; found 574.3867.

5.1.21. 3-(3-(3-(3-(3-(10,11-Dihydro-5*H*-dibenzo[*b*,*f*]azepine-5-yl)propoxy)propoxy)propyl)-10,11-dihydro-5*H*-dibenzo[*b*,*f*]azepine-5-yl)-*N*,*N*-dimethylpropane-1-amine, 21

The product was synthesized according to general procedure D, and was isolated as light yellow oil in 93% yield (0.031 g; 0.0491 mmol). R_f (CH_2Cl_2/CH_3OH 15:1) 0.48. ^{1}H NMR (400 MHz, $CDCl_3$) δ_H 7.17–7.05 (m, 9H), 7.00 (d, 1H, J = 7.7 Hz), 6.94–6.88 (m, 4H), 6.74 (dt, 1H, J = 9.2, 4.6 Hz), 3.84 (t, 2H, J = 6.8 Hz), 3.77 (t, 2H, J = 6.9 Hz), 3.51–3.39 (m, 6H), 3.37 (t, 2H, J = 6.4 Hz), 3.20–3.07 (m, 8H), 2.60 (t, 2H, J = 6.4 Hz), 2.31 (t, 2H, J = 6.4 Hz), 2.16 (s, 6H), 1.83 (dquint, 6H, J = 12.8, 6.4 Hz), 1.77–1.67 (m, 2H). ^{13}C NMR (100 MHz, $CDCl_3$) δ_C 148.4, 140.3, 134.7, 134.3, 131.4, 129.9, 129.8, 126.5, 126.4, 122.5, 120.1, 70.3, 68.7, 68.0, 67.9, 57.9, 49.0, 47.7, 45.7, 32.4, 32.3, 32.1, 31.6, 30.3, 28.4, 26.4. HRMS (ES+): Calcd for $C_{42}H_{49}N_3O_2H$: 628.4216 found 628.4220

5.1.22. 3-(5-(3-(Dimethylamino)propyl)-10,11-dihydro-5*H*-dibenzo[*b*,*f*]azepine-3-yl)prop-2-yn-1-ol 22

p-Toluenesulfonic acid (0.296 g; 1.56 mmol; 1.9 equiv) was added to a solution of **3** (0.343 g; 0.820 mmol; 1 equiv) dissolved in methanol (8.5 mL). After 2 h the reaction had run to completion and was quenched with saturated $NaHCO_{3(aq)}$ before methanol was evaporated. The residue was diluted with H_2O and the aqueous phase was extracted with dichloromethane. The combined organic phases were dried over magnesium sulfate, filtered and evaporated. The product was purified by column chromatography (first dichloromethane/methanol 50:1 then dichloromethane/methanol 10:1) and isolated as brown oil in 72% yield (0.196 g; 0.587 mmol). R_f (dichloromethane/methanol 10:1) 0.29. ^{1}H NMR (400 MHz, $CDCl_3$) δ_H 7.19–7.02 (m, 4H), 7.02–6.89 (m, 3H), 4.41 (s, 2H), 3.72 (t, J = 6.8 Hz, 2H), 3.45 (s, 1H), 3.13 (s, 4H), 2.33 (t, J = 7.4 Hz, 2H), 2.16 (s, 6H), 1.79–1.68 (qv, J = 6.8 Hz, 2H) ppm. ^{13}C NMR (100 MHz, $CDCl_3$) δ_C 148.1, 148.0, 134.9, 134.2, 130., 129.5, 126.6, 125.4, 123.1, 123.0, 120.8, 120.4, 87.4, 85.1, 57.5, 51.0, 48.8, 45.2, 32.6, 31.7, 25.8 ppm. HRMS (ES+): Calcd for $C_{22}H_{26}N_2OH$: m/z 335.2123; found m/z 335.2160.

5.1.23. *N*,*N*-Dimethyl-3-(3-((triisopropylsilyl)ethynyl)-10,11-dihydro-5*H*-dibenzo[*b*,*f*]azepine-5-yl)propane-1-amine, 25

In a glove box with argon atmosphere clomipramine (100.0 mg, 0.285 mmol, 1 equiv), (triisopropylsilyl)acetylene (104.0 mg, 0.569 mmol, 2 equiv), Cs_2CO_3 (0.231 g, 0.712 mmol, 2.5 equiv), acetonitrile (1 mL) and XPhos-precatalyst PdG1 (6.31 mg, 0.0085 mmol, 3%) were all mixed in a vial. Subsequently the vial was closed, removed from the glove box and the reaction mixture was stirred in a preheated heating block at 85 °C. After 7 h the reaction was allowed to cool to room temperature, diluted with $NaHCO_3$ 10% (10 mL) and extracted with ethyl acetate. The combined organic phases were dried over $MgSO_4$, filtered and evaporated. The crude product was purified by flash column chromatography (Dichloromethane followed by 5% methanol in dichloromethane) to yield compound **26** as brown oil (128.1 mg, 87%). R_f (5% methanol in dichloromethane) 0.41. ^{1}H NMR (400 MHz, $CDCl_3$): δ 7.20–6.87 (m, 7H) 3.77 (t, 2H, J = 8.0 Hz) 3.12 (s, 4H) 2.48 (t, 2H, J = 7.4 Hz) 2.27 (d, 6H) 1.82 (quint. 2H, J = 8 Hz) 1.13 (s, 21H, (triisopropylsilyl)). ^{13}C NMR (100 MHz, $CDCl_3$): δ 148.5 148.3, 135.2, 135.0, 130.6–120.8, 107.9 90.1, 57.8, 49.1, 45.4, 33.0, 32.4, 25.7, 19.4, 12.0. MS

5.1.24. 3-(3-ethynyl-10,11-dihydro-5*H*-dibenzo[*b*,*f*]azepin-5-yl)-*N*,*N*-dimethylpropan-1-amine 23

TBAF in THF (1.0 M, 0.15 mL) was added dropwise over a period of 5 min to a solution of **25** (76.3 mg, 0.166 mmol, 1 eq) in THF (1.65 mL) at 0 °C under a N_2 atmosphere. The reaction was stirred for 24 h before the solution was diluted with dichloromethane (50 mL), washed with 10% $NaHCO_3$, dried over $MgSO_4$, filtered and evaporated. The crude product was purified by flash column chromatography (ethyl acetate followed by 2.5% methanol in dichloromethane followed by 5.0% methanol in dichloromethane followed by 10.0% methanol in dichloromethane) to yield **24** as brown oil (60.5 mg, 83%) R_f (Methanol/Ethyl acetate 1:1) 0.23. ^{1}H NMR (400 MHz, $CDCl_3$): δ 7.25–6.90 (m, 7H) 3.77 (t, 2H, J = 6 Hz) 3.14 (s, 4H) 3.01 (s, 1H) 2.42 (t, 2H, J = 8 Hz) 2.23 (s, 6H) 1.79 (quint, 2H, J = 8 Hz). ^{13}C NMR (100 MHz, $CDCl_3$): δ 146.9 146.8, 133.7, 129.2–118.9, 82.8, 75.2, 56.3, 47.5, 44.0, 31.5, 30.6, 24.3. HRMS (ES+): Calcd for $C_{21}H_{24}N_2H$: 305.2018 m/z, found m/z: 305.2045.

5.1.25. 3-(5-(3-(Dimethylamino)propyl)-10,11-dihydro-5*H*-dibenzo[*b*,*f*]azepine-3-yl)propane-1-ol, 24

The product **24** was hydrogenated following general procedure D, and was isolated as yellow oil in 93% yield (0.087 g; 0.256 mmol). R_f (CH_2Cl_2/CH_3OH 10:1) 0.31. ^{1}H NMR (400 MHz, $CDCl_3$) δ_H 7.17–7.05 (m, 3H), 7.01 (d, 1H, J = 7.7 Hz), 6.97–6.86 (m, 2H), 6.76 (d, 1H, J = 7.6 Hz), 3.78 (t, 2H, J = 7.0 Hz), 3.59 (t, 2H, J = 6.4 Hz), 3.15 (s, 4H), 2.64 (t, 2H, J = 7.6 Hz), 2.34 (t, 2H, J = 7.2 Hz), 2.17 (s, 6H), 1.85 (quint, 2H, J = 8.0 Hz), 1.75 (quint, 2H, J = 7.2 Hz). ^{13}C NMR (100 MHz, $CDCl_3$) δ_C 148.6, 147.9, 140.1, 134.6, 131.3, 129.9, 129.7, 126.4, 122.5, 122.4, 120.1, 61.7, 57.7, 49.0, 45.5, 34.3, 32.3, 32.0, 31.9, 26.2. HRMS (ES+): Calcd for $C_{22}H_{30}N_2OH$: 339.2436; found 339.2429.

Acknowledgement

B.S. and H.K. gratefully thank The Danish Council for Independent Research Natural Sciences and the Lundbeck, Carlsberg Foundations and the Alfred Benzon Foundation for financial support along with the Danish Center for Scientific Computing for access to supercomputing facilities. S.S. gratefully thanks the Lundbeck Foundation for financial support.

Supplementary data

Supplementary data associated with this article can be found, in the online version, at http://dx.doi.org/10.1016/j.bmc.2016.04.039.

References and notes

1. Andersen, J.; Kristensen, A. S.; Bang-Andersen, B.; Strømgaard, K. *Chem. Commun.* **2009**, 3677.
2. Kristensen, A. S.; Andersen, J.; Jørgensen, T. N.; Eriksen, J.; Løland, C. J.; Strømgaard, K. *Pharmacol. Rev.* **2011**, *63*, 585.
3. Wong, D. T.; Perry, K. W.; Bymaster, F. P. *Nat. Rev. Drug Disc.* **2005**, *4*, 764.
4. Stahl, S. M. *Essential Psychopharmacology: the Prescriber's Guide: Antipsychotics and Mood Stabilizers*; Cambridge University Press: New York, 2006.
5. Torres, G. E.; Gainetdinov, R. R.; Caron, M. G. *Nat. Neurosci.* **2003**, *4*, 13.
6. Yamashita, A.; Singh, S. K.; Kawate, T.; Jin, Y.; Gouaux, E. *Nature* **2005**, *437*, 215.
7. Singh, S. K. *Channels* **2008**, *2*, 380.
8. Wang, C.-I. A.; Lewis, R. J. *Biochem. Pharmacol.* **2010**, *79*, 1083.
9. Sinning, S.; Musgaard, M.; Jensen, M.; Severinsen, K.; Celik, L.; Koldsøe, H.; Meyer, T.; Bols, M.; Jensen, H. H.; Schiøtt, B.; Wiborg, O. *J. Biol. Chem.* **2010**, *285*, 8363.
10. Andersen, J.; Taboureau, O.; Hansen, K. B.; Olsen, L.; Egebjerg, J.; Strømgaard, C.; Kristensen, A. S. *J. Biol. Chem.* **2009**, *284*, 10276.
11. Koldsø, H.; Severinsen, K.; Tran, T. T.; Celik, L.; Jensen, H. H.; Wiborg, O.; Schiøtt, B.; Sinning, S. *J. Am. Chem. Soc.* **2010**, *132*, 1311.
12. Severinsen, K.; Koldsø, H.; Thorup, K. A. V.; Schjøth-Eskensen, C.; Møller, P. T.; Wiborg, O.; Jensen, H. H.; Sinning, S.; Schiøtt, B. *Mol. Pharmacol.* **2014**, *85*, 208.

13. Andersen, J.; Stuhr-Hansen, N.; Zachariassen, L. G.; Koldsø, H.; Schiøtt, B.; Strømgaard, K.; Kristensen, A. S. *Mol. Pharmacol.* **2014**, *85*, 703.
14. Severinsen, K.; Kraft, J. F.; Koldsø, H.; Vinberg, K. A.; Rothman, R. B.; Partilla, J. S.; Wiborg, O.; Blough, B.; Schiøtt, B.; Sinning, S. *ACS Chem. Neurosci.* **2012**, *3*, 693.
15. Koldsø, H.; Autzen, H. E.; Grouleff, J.; Schiøtt, B. *PLoS One* **2013**, *8*, e63635.
16. Celik, L.; Sinning, S.; Severinsen, K.; Hansen, C. G.; Møller, M. S.; Bols, M.; Wiborg, O.; Schiøtt, B. *J. Am. Chem. Soc.* **2008**, *130*, 2542.
17. Koldsø, H.; Christiansen, A. B.; Sinning, S.; Schiøtt, B. *ACS Chem. Neurosci.* **2013**, *4*, 295.
18. Wang, H.; Goehring, A.; Wang, K. H.; Penmatsa, A.; Ressler, R.; Gouaux, E. *Nature* **2013**, *503*, 141.
19. Penmatsa, A.; Wang, K. H.; Gouaux, E. *Nature* **2013**, *503*, 85.
20. Plenge, P.; Shi, L.; Beuming, T.; Te, J.; Newman, A. H.; Weinstein, H.; Gether, U.; Loland, C. J. *J. Biol. Chem.* **2012**, *287*, 39316.
21. Singh, S. K.; Yamashita, A.; Gouaux, E. *Nature* **2007**, *448*, 952.
22. Plenge, P.; Gether, U.; Rasmussen, S. G. *Eur. J. Pharmacol.* **2007**, *567*, 1.
23. Loland, C. J.; Plenge, P.; Shi, L.; Zhang, P.; Javitch, J. A.; Newman, A. H.; Weinstein, H.; Gether, U. *Basic Clin. Pharmacol. Toxicol.* **2010**, *107*, 116.
24. Plenge, P.; Mellerup, E. T.; Laursen, H. *Eur. J. Pharm.* **1991**, *206*, 243.
25. Susheck, S. J.; Wong, A. L.; Koeller, K. M.; Boehr, D. D.; Draker, K.; Sears, P.; Wright, G. D.; Wong *J. Am. Chem. Soc.* **2000**, *122*, 5230.
26. Bach, A.; Chi, C. N.; Pang, G. F.; Olsen, L.; Kristensen, A. S.; Jemth, P.; Strømgaard, K. *Angew. Chem., Int. Ed.* **2009**, *48*, 9685.
27. Chan, K.-F.; Zhao, Y.; Burkitt, B. A.; Wong, I. L. K.; Chow, L. M. C.; Chan, T. H. *J. Med. Chem.* **2006**, *49*, 6742.
28. Kramer, R. H.; Karpen, J. W. *Nature* **1998**, *398*, 710.
29. Tian, L.; Heyduk, T. *Biochemistry* **2009**, *48*, 264.
30. Schmitt, K. C.; Mamidyala, S.; Biswas, S.; Dutta, A. K.; Reith, M. E. A. *J. Neurochem.* **2010**, *112*, 1605.
31. Banala, A. K.; Zhang, P.; Plenge, P.; Cyriac, G.; Kopajtic, T.; Katz, J. L.; Loland, C. J.; Newman, A. H. *J. Med. Chem.* **2013**, *56*, 9709.
32. Celik, L.; Schiøtt, B.; Tajkhorshid, E. *Biophys. J.* **2008**, *94*, 1600.
33. Christensen, H.; Schjøth-Eskesen, C.; Jensen, M.; Sinning, S.; Jensen, H. H. *Chem. Eur. J.* **2011**, *17*, 10618.
34. Zhou, Z.; Zhen, J.; Karpowich, N. K.; Goetz, R. M.; Law, C. J.; Reith, M. E. A.; Wang, D.-N. *Science* **2007**, *317*, 1390.
35. Zhou, Z.; Zhen, J.; Karpowich, N. K.; Law, C. J.; Reith, M. E. A.; Wang, D.-N. *Nat. Struct. Mol. Biol.* **2009**, *16*, 652.
36. Singh, S.; Piscitelli, C. L.; Yamashita, A.; Gouaux, E. *Science* **2008**, *322*, 1655.
37. Quick, M.; Winther, A. L.; Shi, L.; Nissen, P.; Weinstein, H. *PNAS* **2009**, *106*, 5563.
38. Shi, L.; Quick, M.; Zhao, Y.; Weinstein, H.; Javitch, J. A. *Mol. Cell* **2008**, *30*, 667.
39. Plenge, P.; Mellerup, E. *Eur. J. Pharmacol.* **1985**, *119*, 1.
40. Biessen, E. A.; Norder, J. A.; Horn, A. S.; Robillard, G. T. *Biochem. Pharmacol.* **1988**, *37*, 3959.
41. Torborg, C.; Huang, J.; Schulz, T.; Schäffner, Zapf A.; Spannenberg, A.; Börner, A.; Beller, M. *Chem. Eur. J.* **2009**, *15*, 1329.
42. Littke, A. F.; Fu, G. C. *Angew. Chem., Int. Ed.* **2002**, *41*, 4176.
43. Merkul, E.; Oeser, T.; Muller, T. J. J. *Chem. Eur. J.* **2009**, *15*, 5006.
44. Lee, D. H.; Lee, Y. H.; Harrowfield, J. M.; Lee, I. M.; Lee, H. I.; Lim, W. T.; Kim, Y.; Jin, M. J. *Tetrahedron* **2009**, *65*, 1630.
45. Gelman, D.; Buchwald, S. L. *Angew. Chem., Int. Ed.* **2003**, *42*, 5993.
46. XPhos pre-catalyst (PdG1) was used instead of using separate phosphine and palladium source, see Ref. 42.
47. Chen, J. G.; Rudnick, G. *Proc. Natl. Acad. Sci. U.S.A.* **2000**, *97*, 1044.
48. Henry, L. K.; Field, J. R.; Adkins, E. M.; Parnas, M. L.; Vaughan, R. A.; Zou, M.-F.; Newman, A. H.; Blakely, R. D. *J. Biol. Chem.* **2006**, *281*, 2012.
49. Thompson, B. J.; Jessen, T.; Henry, L. K.; Field, J. R.; Gamble, K. L.; Gresch, P. J.; Carneiro, A. M.; Horton, R. E.; Chisnell, P. J.; Belova, Y.; McMahon, D. G.; Daws, L. C.; Blakely, R. D. *Proc. Natl. Acad. Sci. U.S.A.* **2011**, *108*, 3785.
50. Bright, S. A.; Brinkø, A.; Larsen, M. T.; Sinning, S.; Williams, D. C.; Jensen, H. H. *Bioorg. Med. Chem. Lett.* **2013**, *23*, 1220.
51. Sali, A.; Blundell, T. L. *Mol. Biol.* **1993**, *234*, 779.
52. Fiser, A.; Do, R. K.; Scaronali, A. *Protein Sci.* **2000**, *9*, 1753.
53. Beuming, T.; Shi, L.; Javitch, J. A.; Wein, N. H. *Mol. Pharmacol.* **2006**, *70*, 1630.
54. Koldsø, H.; Severinsen, K.; Tran, T. T.; Celik, L.; Jensen, H. H.; Wiborg, O.; Schiott, B.; Sinning, S. *J. Am. Chem. Soc.* **2010**, *132*, 1311.
55. Kalé, L.; Skeel, R.; Bhandarkar, M.; Brunner, R.; Gursoy, A.; Krawetz, N.; Phillips, J.; Shinozaki, A.; Varadarajan, K.; Schulten, K. *J. Comput. Phys.* **1999**, *151*, 283.
56. Philips, J. C.; Braun, R.; Wang, W.; Gumbart, J.; Tajkhorshid, E.; Villa, E.; Chipot, C.; Skeel, R. D.; Kalé, L.; Schulten, K. *J. Comput. Chem.* **2005**, *26*, 1781.
57. MacKerell, A. D. J.; Bashford, D.; Bellott, M.; Dunbrack, R. L., Jr.; Evanseck, J. D.; Field, M. J.; Fischer, S.; Gao, J.; Guo, H.; Ha, S.; Joseph-McCarthy, D.; Kuchnir, L.; Kuczera, K.; Lau, F. T. K.; Mattos, C.; Michnick, S.; Ngo, T.; Nguyen, D. T.; Prodhorn, B.; Reiher, W. E., III; Roux, B.; Schlenkrich, M.; Smith, J. C.; Stote, R.; Straub, J.; Watanabe, M.; Wiorkiewicz-Kuczera, J.; Yin, D.; Karplus, M. *J. Phys. Chem. B* **1998**, *102*, 3586.
58. MacKerell, A. D.; Feig, M.; Brooks, C. L., III *J. Comput. Chem.* **2004**, *24*, 1400.
59. Darden, T.; York, D.; Pedersen, L.; Ewald, Particle mesh *J. Chem. Phys.* **1993**, *98*, 10089.
60. Feller, S. E.; Zhang, Y.; Pastor, R. W.; Brooks, B. R. *J. Chem. Phys.* **1995**, *103*, 4613.
61. Kalé, L.; Skel, R.; Bhandakar, M.; Brunner, R.; Gursoy, A.; Krawetz, N.; Phillips, J.; Shinozaki, A.; Varadarajan, k.; Schulten, K. *J. Comput. Phys.* **1999**, *151*, 283.
62. Celik, L.; Schiott, B.; Tajkhorshid, E. *Biophys. J.* **2008**, *94*, 1600.
63. Sherman, W.; Day, T.; Jacobson, M. P.; Friesner, R. A.; Farid, R. *J. Med. Chem.* **2006**, *49*, 534.
64. Suite 2011: Schrödinger Suite 2011 Induced Fit Docking protocol; Glide Version 5.7, Schrödinger, LLC, New York, NY, 2011; Prime Version 2.2, Schrödinger, LLC, New York, NY, 2011.
65. Friesner, R. A.; Murphy, R. B.; Repasky, M. P.; Frye, L. L.; Greenwood, J. R.; Halgren, T. A.; Sanschagrin, P. C.; Mainz, D. T. *J. Med. Chem.* **2006**, *49*, 6177–6196.
66. Cheng, Y.; Prusoff, W. H. *Biochem. Pharmacol.* **1973**, *22*, 3099.